BIOFUELS PRODUCTION USING STARCH OVER HETEROGENEOUS CATALYSTS

A Thesis Submitted to
The Graduate School of Engineering and Sciences of
İzmir Institute of Technology
in Partial Fulfillment of the Requirements for the Degree of

MASTER OF SCIENCE

in Chemical Engineering

by
Merve UÇAROĞLU

July 2017
İZMİR

We approve the thesis of **Merve UÇAROĞLU**

Examining Committee Members:

_____

Prof. Dr. Erol ŞEKER
Department of Chemical Engineering, İzmir Institute of Technology

_____

Assoc. Prof. Dr. Ekrem ÖZDEMİR
Department of Chemical Engineering, İzmir Institute of Technology

_____

Prof. Dr. Oğuz BAYRAKTAR
Department of Chemical Engineering, Ege University

21 July 2017

_____

Prof. Dr. Erol ŞEKER
Supervisor, Department of Chemical Engineering
İzmir Institute of Technology

_____

Prof. Dr. Fehime ÇAKICIOĞLU ÖZKAN
Head of the Department of Chemical

_____

Prof. Aysun SOFUOĞLU
Dean of the Graduate School of Engineering and Sciences

ACKNOWLEDGEMENTS

Foremost, I would like to express my sincere gratitude to my MSc supervisor Prof. Dr. Erol ŞEKER for the continuous support of my MSc study and research, for his patience, motivation, enthusiasm, and immense knowledge, without whom this thesis would not have been written.

Beside my MSc supervisor, I would like to thank Okan AKIN and Filiz KURUCAOVALI for their technical supports. I would like to thank Prof. Dr. Selahattin YILMAZ for his help too.

My sincere thanks also go to Bertan ÖZDOĞRU, Berk TÜRKKUL and Özgün DELİİSMAİL for all their help throughout the study in the lab.

Last but not the least, I would like to thank my family and all my friends supporting me spiritually throughout the study.

ABSTRACT

BIOFUELS PRODUCTION USING STARCH OVER HETEROGENEOUS CATALYSTS

In this study, the effect of acidity and acidic strength on the product distribution in the hydrolysis of starch was investigated on mixed oxide supported Ni catalysts prepared using different types of metal oxides with varying compositions and, the calcination temperatures. SiO_2/Al_2O_3 (mass ratios of 30/70, 50/50, 70/30) and ZnO/TiO_2 (mass ratios of 10/90, 30/70, 50/50) catalysts were synthesized using a sol-gel method. For all the ratios and metal oxide types, Ni weight loading was 1%, 5.5% and 10%. The calcination temperatures used for all the SiO_2/Al_2O_3 catalysts were 500 ^oC, 700 ^oC and 900 ^oC. The calcination temperatures used for all the ZnO/TiO_2 catalysts were 300 ^oC, 400 ^oC and 500 ^oC. The starch hydrolysis reaction was carried out at 90 ^oC for the reaction time of 24 h. The concentration of the products was determined using HPLC and acidity/acidic strength of the catalyst were measured using NH_3-TPD.

This study showed that the product distribution was affected by catalyst compositions and calcination temperatures that resulted varying total acidity and acidic strength. Unidentifiable saccharides, maltotriose, xylose, and glucose were produced during the hydrolysis of starch on all the SiO_2/Al_2O_3 supported Ni catalysts while there were only unidentifiable saccharides on all the ZnO/TiO_2 supported Ni catalysts. The products distribution was found to strongly dependent on the nature of the acid type; for instance, $Al_2(SO_4)_3$ crystalline phase was more active than the acid type on ZnO and TiO_2 anatase crystalline phases. In addition, the glucose yield increased on the large $Al_2(SO_4)_3$ crystallite sizes, e.g. the catalyst having 42 nm of $Al_2(SO_4)_3$ crystallite size gave ~15% glucose yield whereas that having 10.5 nm of $Al_2(SO_4)_3$ crystallite size gave 0%. Besides, acidic strength was more important than total acidity for the same acid type. In fact, the lower the acidic strength, such as located at 150 ^oC, higher the glucose yield was obtained.

ÖZET

KATI KATALİZÖRLER ÜZERİNDE NİŞASTA KULLANILARAK BİYOYAKIT ÜRETİMİ

Bu çalışmada, nişasta hidrolizinde asitliğin ve asidik kuvvetin ürün dağılımı üzerindeki etkisi, çeşitli bileşimlerdeki metal oksitler ve kalsinasyon sıcaklıkları kullanılarak hazırlanan karışık oksit destekli Ni katalizörleri üzerinde araştırılmıştır. SiO_2/Al_2O_3 (kütle oranları: 30/70, 50/50, 70/30) ve ZnO/TiO_2 (kütle oranları: 10/90, 30/70, 50/50) katalizörleri sol-jel yöntemi kullanılarak sentezlenmiştir. Tüm oranlar ve metal oksit türleri için Ni yükü yüklemesi %1, %5.5 ve %10 idi. Tüm SiO_2/Al_2O_3 katalizörleri için kullanılan kalsinasyon sıcaklıkları 500 ^oC, 700 ^oC ve 900 ^oC idi. Tüm ZnO/TiO_2 katalizörleri için kullanılan kalsinasyon sıcaklıkları 300 ^oC, 400 ^oC ve 500 ^oC idi. Nişasta hidroliz reaksiyonu, 24 saatlik reaksiyon süresi boyunca 90 ^oC'de gerçekleştirildi. Ürünlerin konsantrasyonu HPLC kullanılarak belirlendi ve katalizörün asitliği/ asidik kuvveti NH_3-TPD kullanılarak ölçüldü.

Bu çalışma, ürün dağılımının, değişen toplam asitlik ve asidik kuvvet ile sonuçlanan katalizör bileşimleri ve kalsinasyon sıcaklıklarından etkilendiğini gösterdi. Tanımlanamayan sakkaritler, maltotrioz, ksiloz ve glikoz, tüm SiO_2/Al_2O_3 destekli Ni katalizörleri üzerinde nişasta hidrolizi sırasında üretilirken, tüm ZnO/TiO_2 destekli Ni katalizörleri üzerine sadece tanımlanamayan sakkaritler mevcuttu. Ürün dağılımının asit türüne son derece bağlı olduğu bulundu. Örneğin, $Al_2(SO_4)_3$ kristal fazı ZnO ve TiO_2 anataz kristal fazlarındaki asit türünden daha aktifti. Ek olarak, glikoz verimi, büyük $Al_2(SO_4)_3$ kristalit boyutlarında, ör. 42 nm $Al_2(SO_4)_3$ kristalit boyutuna sahip olan katalizör ~%15 glikoz verimi verirken, 10.5 nm $Al_2(SO_4)_3$ kristalit boyutuna sahip olan katalizör %0 verimi verdi. Ayrıca, aynı asit türünün asidik kuvveti toplam asitliğinden daha önemliydi. Aslında, 150 ^oC'de bulunan gibi asidik kuvvet ne kadar düşük olursa, glikoz verimi de artar.

TABLE OF CONTENTS

LIST OF FIGURES

Figure **Page**

LIST OF TABLES

Table **Page**

CHAPTER 1

INTRODUCTION

Population of the world which was 7.0 billion in 2012 is expected to be 9.0 billion in 2040 (World Energy Outlook 2014). This fast growing world population accompanying vastly increased human daily activities have resulted in constantly growing energy demand. In addition, the industrialization has increased energy demand, too (Kiran et al., 2014). World primary energy demand have been estimated increase to be 4929 million tons of oil equivalent between 2012 and 2040 according to New Policies Scenario. (World Energy Outlook 2014). Fuel types of world primary energy demand in the New Policies Scenario are given in Figure 1. It is seen that the demand on renewable fuels increase faster than that of any other fuels.

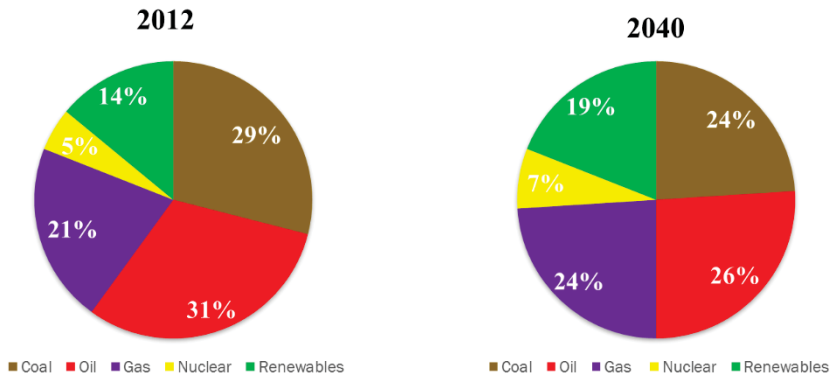

Figure 1. Fuel shares of world primary energy demand in the New Policies Scenario (Source: World Energy Outlook 2014).

There are several factors which affect this increased demand. One of the factors is to provide economic sustainability (Kiran et al., 2014). The use of fossil fuel is crucial for the global energy demand accounting for more than 80% of the world primary consumption (Mohr et al., 2015). Because all the fossil fuels are non-renewable sources (Perez et al., 2014), diminishing fossil fuel sources will create a global energy crisis for present and future (Patel et al., 2017). Therefore, the global community concentrate on searching renewable energy sources to find a viable solution for the depletion of fossil fuel resources in the future (Shafiee and Topal., 2008).

Another factor of this increased demand on renewable energy is global awareness on environmental issues, such as increased air pollution (Patel et al. 2017). It has led to the Paris Agreement on climate change which brought many countries together, even the countries attributing the most to the world greenhouse gas emissions (World Energy Outlook 2016). One of the major aims of international climate policy is to limit global warming to below 2 ^{o}C (CCPI 2017).

Global warming is the most significant environmental problem that the world has ever been facing. Greenhouse gases, such as CO_2, CH_4, NO_x, N_2O, cause global warming and acids rain. (Iwata and Okata., 2014). In fact, greenhouse gas emissions were composed of carbon dioxide (76%), methane (16%), nitrous oxide (6%), F-gases (2%) (IPCC 2014). The main source of greenhouse gases is the usage of fossil fuel. In contrast to fossil fuels, renewable energy sources are much cleaner and seem to be viable solutions for decreasing greenhouse gas emissions and real problems, such as environmental and mankinds' health (Kiran et al., 2014). Transportation is a vital component of economic and social activities, which pave the way to the development of poor economies. In fact, the development of transport and mobility are crucial for countries to have more sustainable development since they enhance economic activities through moving people from places to places and distributing goods and services around the world (Sousa et al., 2015).

Among the renewable energy sources, biofuels seem to be the most sustainable energy carriers. They could be utilized as transportation fuel directly in the engines or indirectly with some modification to the engines (Kiran et al.,2014). Unfortunately, high production cost of biofuels is major road block for them to be substitute for the petroleum derivative fuels. Therefore, many researchers around the world have been working on reducing the production cost of biofuels to make these fuels more attractive. In addition, may governments in developed and developing countries have been encouraging investment incentives for the use of biofuels through the financial assistance, legal obligations to further reduce the production cost of biofuels (Kiran et al., 2014).

Biofuel can be produced from biomass (oils, fats, cellulose, hemicellulose, and starch) and biomass derivatives. Types of biofuels are highly dependent on biomass type. For instance, biodiesel is produced by esterification/transesterification of oils/fats or "Green diesel" (also known as renewable diesel) is produced using oils/fats, cellulose, hemicellulose. Other examples are dimethyl ether produced using

cellulose/hemicelluloses and ethanol/butanol produced using starch or saccharides. Possible pathways of biofuels productions are given in Figure 2 (Babu et al. ,2014).

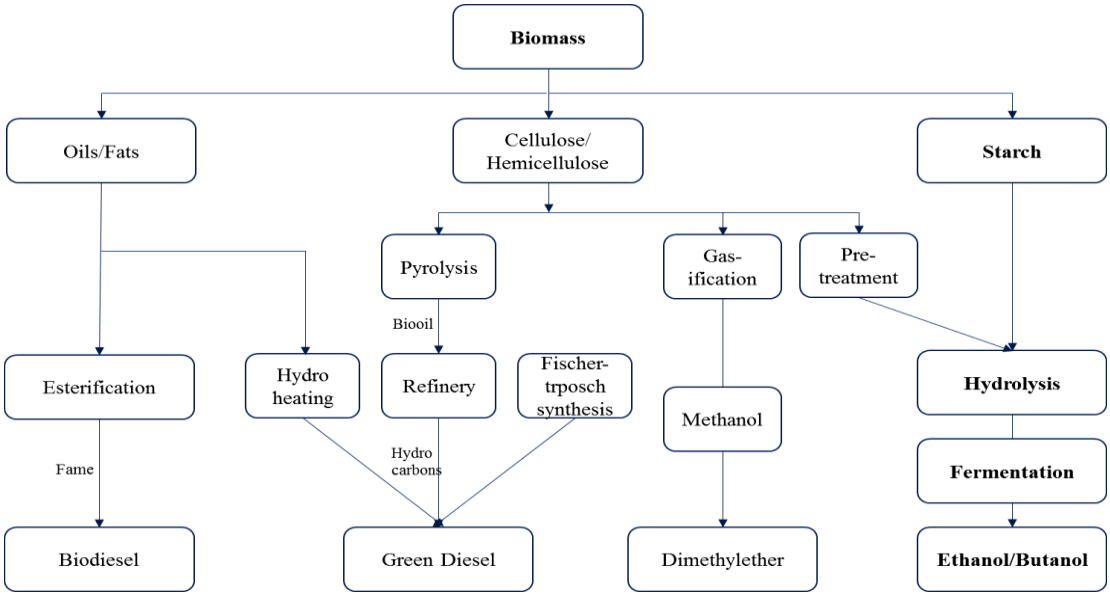

Figure 2. Possible production pathways for biofuels
(Source: Babu et al., 2014).

Ethanol (bioethanol) is used as an alternative fuel in internal combustion engines (Trindade and Santos., 2017). Also, ethanol is used to produce ethylene and ethylene glycol as a valuable chemical and to decrease aromatic emissions and CO (Isıkgor and Becer.,2015). Butanol is also used as an alternative fuel in internal combustion engines. It could be mixed with gasoline as well as diesel. Ethanol and butanol are produced by fermentation of starch or cellulose (Trindade and Santos., 2017). Because yeast cannot use starch as a raw material, hydrolysis of starch is needed to obtain fermentable sugars (Zabed et al., 2017).

Starch $(C_6H_{10}O_5)_n$, a polymeric carbohydrate, is the basic component of corn seeds, potato tubers, and the roots and stems of other plants (Janssen and Moscicki, 2009). D-glucose ($C_6H_{12}O_6$) is the building unit of the starch granules which varies from 1 µm to 100 µm in diameter (Thomas and Atwell, 1997). It includes 70-80 % amylopectin and 20-30% amylose (BeMiller and Whistler., 2009). The arrangement of amylopectin and amylose is well ordered inside starch granule. If starch is heated in water for a while, the ordered arrangement is destroyed; thus, resulting in hydrolysis. (Janssen and Moscicki, 2009)

Hydrolysis means the cleavage of chemical bonds, that hold the glucose molecules, by the addition water (Stoker H., 2017). In starch hydrolysis reaction pathway, dextrin is the first product, maltose is the second product, and glucose is the final product. Hydrolysis reaction of starch is very slow. Therefore, acids or enzymes are needed to accelerate the hydrolysis reaction (Janssen and Moscicki, 2009).

Acidic hydrolysis of starch has been a commercial method to produce glucose since 1814 (Lorenz and Johnson., 1972). For example, sulfuric acid (H_2SO_4) is commonly used as homogeneous acid for starch hydrolysis. However, in such acid hydrolysis processes, there are some problems, such as the necessity of acid recovery after hydrolysis, waste treatment and, reactor corrosion. Therefore, homogeneous acid hydrolysis is not the first choice for a process development if there are alternatives (Huang and Fu., 2013).

Enzymatic hydrolysis of starch is also another commercial method. Enzyme catalyzed hydrolysis is carried out in two steps. First step is liquefaction in which starch degrades into dextrins. Second step is saccharification in which the dextrins decomposes into glucose. However, for enzymatic hydrolysis of starch, there are some drawbacks, such as the requirement of high temperatures, extra equipment high initial investment cost and the cost of the enzymes (Sheng-Xu et al., 2016 and Dhepe et al., 2005).

Heterogeneous hydrolysis is more feasible alternative to homogeneous and enzymatic hydrolysis. There are some advantages, such as lower cost of catalyst per unit of production, easier catalyst separation and easy control of the reaction (Zajsek and Gorsek., 2010). Also, the use of heterogeneous catalysts decreases equipment corrosion and ensures safe catalyst handling (Iloukhani et al., 2002). Therefore, the use of heterogeneous catalysts is a viable solution for catalytic hydrolysis of starch.

In this study, the effects of acidity and acidic strength on the starch hydrolysis product distribution was investigated using the mixed oxides supported Ni catalysts. The acidity and acidic strength of the catalysts were changed using different types of metal oxides, their compositions, and also the calcination temperatures. In this study, SiO_2/Al_2O_3 and ZnO/TiO_2 catalysts were synthesized by sol gel method using mass ratios of 30/70, 50/50, 70/30 and 10/90, 30/70, 50/50 respectively. For all the mixed oxides, Ni weight loading was 1%, 5.5% and 10%. The calcination temperatures used for all the SiO_2/Al_2O_3 catalysts are 500 ^oC, 700 ^oC and 900 ^oC whereas the calcination temperatures used for all ZnO/TiO_2 catalysts were 300 ^oC, 400 ^oC and 500 ^oC. All the catalysts were

used in the starch hydrolysis reaction carried out at 90 ^{o}C for 24 h. The products were analyzed using HPLC and the acidity and acidic strength of the catalysts were determined using NH_3-TPD.

This thesis conists of five chapters. In chapter 1, the general background on the worldwide energy demand and supply is given with the focus on the renewable energy sources. In Chapter 2, the literature review is presented for the characteristics of the sugar, starch, lignocellulosic based feedstocks, the hydrolysis of starch using homogeneous and heterogeneous catalysts This chapter is followed by Materials and Methods chapter to explain in detail the experimental procedures used in this study.. In Chapter 4, the results are presented and discussed to better understand the correlation between the acidity and acidic strength of the catalysts and the product distribution in starch hydrolysis. Finally, conclusions are listed in Chapter 5.

CHAPTER 2

LITERATURE REVIEW

2.1. Sugar, Starch and Lignocellulosic Based Feedstocks

Biofuel can be produced from many biomass resources, such as sugar, starch and lignocellulosic biomass. Conversion of biomass into biofuel is one of the important research topics which depend on the nature of the raw material and strongly related to derivation route of sugar solutions. For example, an extraction process is required for sugar based feedstocks to produce fermentable sugars. Another feedstock, starch must be hydrolyzed to obtain fermentable sugars, while lignocellulosic biomass requires one more step before hydrolysis to convert cellulose structure to obtain fermentable sugars (Zabed et al., 2017). Selection of raw materials for biofuel production is strongly depends on their availability, cost of raw material and process, carbohydrate content of raw materials (Kapdan et al., 2011).

Sugar based feedstocks are sugar cane, sugar beet, and fruit which is used for biofuel production (Balat and Balat, 2009). For example, sugar cane is used as raw material for producing bioethanol in tropical areas such as Brazil, India, and Colombia. However, natural seasonal availability of sugar crops restricts their conversion to biofuel, although they have high sugar yields per acre and favorable cost of sugar conversion (Vohra et al., 2014).

On the other hand, starch based feedstocks are corn, wheat, rice, potatoes, sweet potato and so on (Balat and Balat, 2009). For instance, corn which, includes 60-70% starch, is major raw material used in the industry for bioethanol production (Zabed et al., 2017). This sort of raw material is commonly used in North America and Europe (Vohra et al., 2014). In general, starch based feedstocks are easily available all over the world, and storage of starch is possible for a long time, and high biofuel yield can be obtained (Zabed et al., 2017).

Other type of feedstock is lignocellulosic based feedstocks, which include agricultural residues, grasses, and wood residues (Vohra et al., 2014). These feedstocks have very complex structure because they compose of cellulose and hemicellulose which

are highly resistant to degrade (Zabed et al., 2017). Hydrolysis and a pretreatment step are needed to get high yield of hydrolysis. Therefore, conversion route of lignocellulosic to ethanol is more difficult than sugar and starch (Balat and Balat, 2009).

2.2. Hydrolysis of starch using homogeneous catalysts

Starch hydrolysis is carried out using acids or enzymes. For example, if starch is heated with acid, starch granules are broken down into small molecules, and finally leads to form glucose molecules. The general expression of hydrolysis of starch into glucose molecule shown in below equation.

$$(C6H10O5)n + nH2O = nC6H12O6 \quad (2.1)$$

Starch Water Glucose

In the reaction mechanism, starch granules are first broken down into dextrins (composed of small chains of glucose units). Then, dextrins are broken down into maltose molecules (consisted of two glucose molecules). Finally, maltose molecules are broken down into glucose (Gaman and Sherrington, 1981).

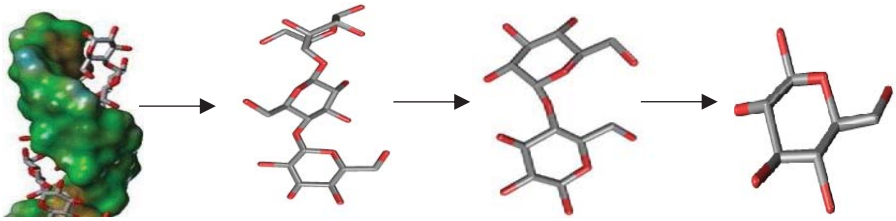

Starch Dextrins Maltose Glucose

Figure 3. Illustration of starch, dextrins, maltose, and glucose molecules. (Source: 3D conformers pictures are taken from Polysac3DB and PubChem).

Starch granule contains mainly amylopectin (70-80%) whereas contains less likely amylose (20-30%) molecule (BeMiller and Whistler, 2009). Also, it includes small amount of proteins, lipids, and minerals (Qi and Tester, 2016).

Amylose is relatively long molecule. It includes 99% α (1-4) linkages and differs in size, polydispersity and structure related to type of starch. In starch hydrolysis, α (1-4) linkages are opened with the aid of catalyst to obtain products (Tester et al., 2004). High amylose content is drawback for starch hydrolysis (Qi and Tester, 2016).

Amylopectin is much larger molecule than amylose. The structure of amylopectin is mostly branched. It includes 95% α (1-4) linkages and 5% α (1-6) linkages. In starch hydrolysis, α (1-4) and α (1-6) linkages open with the help of catalyst to obtain products. Unit chains of amylopectin is shorter than amylose chain. (Tester et al., 2004). Chemical structures of amylose and amylopectin are given in Figure 4.

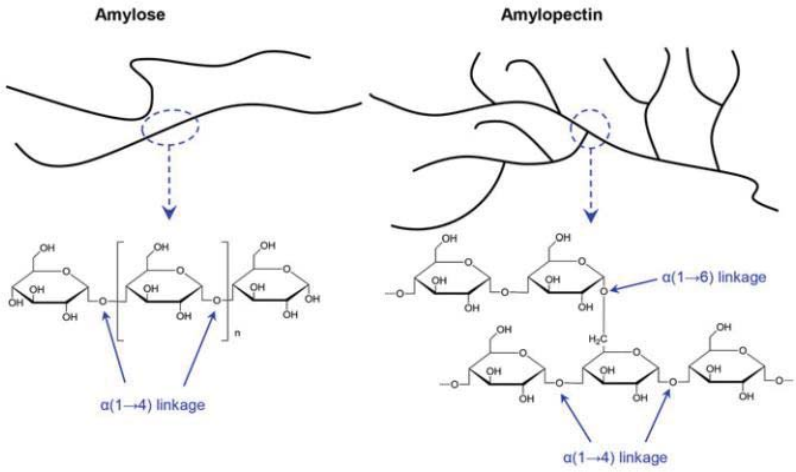

Figure 4. Chemical structures of amylose and amylopectin.
(Source: taken from Xie et al., 2014).

Lipids are found as complexed form with amylose in starch granules. This complex structure causes to resistance hydrolysis. Also, proteins and phosphorous cause to resistance hydrolysis (Tester, et al. 2006).

Catalyst type (acid hydrolysis or enzymatic hydrolysis) affects hydrolysis of starch as a major factor (Khawla et al., 2014). Homogeneous acid catalysts, one of the catalyst types, can be applied for hydrolysis of starch. For instance, phosphoric acid and hydrochloric acid were applied at a range 140-160^{0}C with pH below 2. High dextrose equivalent (DE) syrups (30% of total solids) were produced under this reaction conditions by using phosphoric acid. However, 5-hydroxymethylfurfural, by product was generated. When hydrochloric acid was used, hydrochloric acid generated toxic fumes at this reaction conditions such as higher temperature with lower pH. Therefore, an expensive corrosive-resistant equipment was needed. Furthermore, higher cost ion-exchange resins were needed to desalinate syrup after neutralization under these conditions (Fontane et al., 2008). Enzymatic catalysts can also be applied for hydrolysis of starch. In the study carried out by Tasic et al., enzymatic hydrolysis was investigated at milder conditions compared to homogeneous acid hydrolysis, however, it required two steps (liquefaction

and saccharification). Liquefaction was applied by using amylases enzymes (amylases enzymes open the chemical bond α (1-4) linkages of starch) to convert starch into maltodextrin and maltose at 80-100 ^{0}C. Then, saccharification was applied by using glucoamylase to generate clean glucose than partially hydrolyzed starch in the first step (Khawla et al., 2014). However, using enzymatic catalysts is not an effective solution due to the cost of enzymes and of initial investment (Tasic et al., 2009).

Hydrolysis conditions such as temperature, amount of catalyst, pH, are important parameters on hydrolysis of starch. Also, all these parameters can serve interactive effects on the rate of hydrolysis. Therefore, optimization of these parameters is very useful. For instance, an experimental design was made for temperature range 63-97 ^{0}C, pH 5.6-7.6, enzyme amounts 27.6-372.4 μL/kg, calcium addition 0-120 μg/g, dry weight concentration 3-37% w/w and stirring 0-200 rpm for α-amylolytic hydrolysis of amylopectin potato starch. The best rate was found at dextrose equivalent (the rate of hydrolysis expression) of 10 at 90 ^{0}C (higher temperature) and pH 6. Maximum temperature was found as major parameter due to affected oligosaccharide composition and starch conversion in this survey. It was observed that higher level of calcium and higher level of pH cause to decrease maximum temperature (Marchal et al., 1998).

Besides optimizing hydrolysis conditions, hydrolysis of starch can be integrated with ultrasound to reach higher rate of hydrolysis and higher starch conversion to glucose. For example, hydrolysis of starch was increased by using sulfuric acid catalyst and ultrasound irradiation. This increment was depended on temperature (90-100 ^{0} C) and acid concentration (1-5 wt%). For starch hydrolysis, relative enhancement of % 100 of glucose yield at 90^{0}C and 5 wt% of sulfuric acid concentration by using ultrasound irradiation. For maltose hydrolysis, relative enhancement of 55.56 % of glucose yield (the best among the other temperature and concentration range) with 90^{0}C and 3 wt% of sulfuric acid concentration by using ultrasound irradiation (Choi and Kim, 1994). In addition, hydrolysis of starch can be integrated with a nonthermal technique like ultrahigh pressure. For instance, hydrolysis of starch was increased by using HCl acid catalyst and ultrahigh pressure. This increment was depended on increased HCl concentration (0.1- 4 M) and pressure level (below 400 MPa there was no hydrolysis of corn starch, 600 MPa was required for hydrolysis) (Choi et al., 2009).

2.3. Hydrolysis of starch via heterogeneous catalysts

Heterogeneous catalyst is environmentally friendly (Yamaguchi and Hara, 2010) because it can be separated from solution easily and can be recovered. The use of heterogeneous catalyst is advantageous compared to the use of homogeneous catalyst and enzyme catalyst if glucose is produced from starch with one step reaction (Dhepe et al., 2005). Therefore, several researchers focus on investigating hydrolysis of sucrose, maltose, starch, even cellulose over heterogeneous catalysts.

There are several kinetic studies for hydrolysis of sucrose using heterogeneous catalysts. For example, for sucrose hydrolysis via heterogeneous catalyst, the reaction kinetic and thermodynamic parameters of silica contained 12-tungstophosphoric acids were investigated. It was found that the adsorption of water was low for silica contained 12-tungstophosphoric acid catalyst and stated that it could perform better than hydrophilic catalysts like Al_2O_3 and Nb_2O_5 for hydrolysis of sucrose (Iloukhani et al., 2002). In another study, the reaction kinetic and thermodynamic parameters of V_2O_5/SiO_2 catalyst for sucrose hydrolysis was investigated. The rate constants and activation parameters of catalyst were found out. It was found that the adsorption of water tendency was low for V_2O_5/SiO_2 catalyst whereas SiO_2 exhibited hydrophilic catalyst (Langeroodi et al., 2012). To understand how -COOH groups (as homogeneous and as heterogeneous) affect the kinetics of hydrolysis of sucrose, a comparative kinetic study for homogeneous catalyst (acetic acid) and heterogeneous catalyst (carboxylic cationites) was investigated. The kinetic parameters of catalysts were investigated by DSC data with Friedmann's method and concluded that catalyst efficiency of carboxylic cationites were 5000 times higher than acetic acid (Chambre et al., 2008).

There are many studies describing the catalytic performance of heterogeneous catalysts on hydrolysis of starch and cellulose. For example, a micellar heteropolyacid ($C_{16}H_2PW$) was used for hydrolysis of starch and cellulose. It was reported that starch conversion was increased up to 96.1 %, glucose yield 82.4 %, glucose selectivity 85.7% at 120^0C for 5h with 0.1 g starch. It was found that temperature and reaction time was very effective on hydrolysis of starch. Increasing temperature caused increased conversion and selectivity of starch hydrolysis, such that, starch conversion increased from 75.2 % (at 110^0C for 6h) to 93.7 % (at 130^0C for 2h). Cellulose conversion was increased up to 39.3%, glucose yield 33.5%, glucose selectivity 85.5% at 170^0C for 6h

with 0.1 g cellulose. Increasing reaction temperature caused increment in conversion and selectivity of cellulose hydrolysis (until 180^0C). For instance, the results showed that cellulose conversion was increased from 29.0% (at 160^0C for 8h) to 48.5% (at 180^0C for 8h) glucose selectivity decreases to 80.9%. It was found that heterogeneous catalyst ($C_{16}H_2PW$) showed significant catalytic performance on hydrolysis of starch and cellulose (Cheng et al., 2011). LF (lignosulfonate-based heterogeneous sulfonic catalyst) was prepared that involving -SO_3H, -COOH, -OH groups. These prepared insoluble and sulfonic catalyst exhibited acidic character and high catalytic activity for hydrolysis of starch, maltose, sucrose etc. Glucose yield of starch was 87%, maltose 94 %, and sucrose 98% (150^0C, for 6h, with 0.1 g substrate, 0.1 g catalyst, 5.0 ml H_2O) (Zhang et al., 2013). Besides hydrolysis catalytic performance, some catalysts have catalytic activity for both hydrolysis and dehydration. For instance, starch conversion to HMF was possible by using SO_4^{2-}/ZrO_2-Al_2O_3 synthesized with impregnation method. This catalyst was applied for different Zr/Al molar ratios, water amount, reaction time, catalyst amount and reaction temperature. The effect of acid-base property of SO_4^{2-}/ ZrO_2-Al_2O_3 on starch conversion was investigated (Yang et al., 2012). SO_4^{2-}/ ZrO_2-Al_2O_3 samples were defined here like CSZA-1 (Zr-Al mol ratio of 9:1), CSZA-2 (Zr-Al mol ratio of 7:3), CSZA-3 (Zr-Al mol ratio of 1:1), CSZA-4 (Zr-Al mol ratio of 3:7), and CSZA-5 (Zr-Al mol ratio of 1:9). Decreasing molar ratio leads to increase amounts of base sites and decrease amounts of acid cites (Yan et al., 2009). TRS yield (%) correlated linearly with amount of acid sites (mmol/g) of CZSA catalysts. CZSA-1 (Zr-Al mol ratio of 9:1) had the best activity for the hydrolysis of starch, however, the targeted product was HMF. Therefore, CSZA-3 was found the best among the others with capability of hydrolysis and dehydration due to had high acidity and moderate basicity. Then, catalyst type effect was investigated. Excluding H_2SO_4, the activity of CSZA-3 was the best among the other catalyst (Al_2O_3, Amberlyst-15, Hβ, HZSM-5, HY) with 48% HMF yield, and 1% glucose yield from starch. The other catalysts were not active for HMF and glucose production, however, they were active for TRS at the conditions of 150^oC for 4h. Therefore, prolonged reaction time was needed to test catalysts which have lower activity. It was found that the best condition for CZSA-3 is at temperature of 150^0C for 6h for 55% yield of HFM. (Yang et al., 2012).

The factors affecting the hydrolysis of carbohydrates have been investigated in many aspects. Most investigated factors were type of feedstocks, type of catalysts, temperature of reaction, kinetic and thermodynamic properties of catalysts, and catalytic

performance of heterogeneous catalysts on carbohydrates. However, studies investigating the effect of acidity of heterogeneous catalysts on hydrolysis of starch are rare. Therefore, studies need to be focused on the effect of acidity of metal oxides synthesized by the sol gel method on starch hydrolysis due to their high specific surface area and pore size (Huang and Fu., 2013). In addition, sol gel method is the excellent technique due to capable of controlling composition, homogeneity, and structure of the catalyst in the synthesis of catalyst (Cauqui and Izquierdo, 1992).

CHAPTER 3

MATERIALS and METHOD

3.1. Materials

In this study, two types mixed oxide catalysts were prepared using sol-gel method; Ni/SiO_2-Al_2O_3 with the Ni loadings 1, 5.5, 10 wt % varying SiO_2-Al_2O_3 compositions, such as 30/70 ,50/50 ,70/30 and also using different calcinations temperatures, such as 500 ^oC, 700 ^oC ,900 ^oC. The another mixed oxide catalysts were Ni/ZnO-TiO_2 with the Ni loadings 1, 5.5, 10 wt% prepared with the sol-gel method using different ZnO-TiO_2 compositions, such as 10/90, 50/50, 30/70 and also different calcinations temperatures, such as 300 ^oC, 400 ^oC, 500 ^oC.

In the synthesis of the Ni/SiO_2-Al_2O_3 catalysts, tetraethyl orthosilicate (TEOS) was the precursor for silica and aluminum isopropoxide (AIP) was precursor for alumina. Ethanol (EtOH) and deionized water (DIW) were used as solvents and hydrochloric acid (HCl) and sulfuric acid (H_2SO_4) used as peptizing agent in the sol-gel method. Ni precursor was Ni(II) acetate. Properties of all the chemicals used in the synthesis of the catalysts are given in Table 1 and Table 2.

Table 1. Properties of chemicals used in Aluminum oxide synthesis.

Components	**Molecular weight (g/mol)**	**Density (g/ml)**	**Purity**	**Formula**
Aluminum isopropoxide	204.24	1.035	0.98	$Al(C_3H_7O)_3$
Water	18.02	0.999	1	H_2O
Sulphuric Acid	98.08	1.84	0.9999	H_2SO_4
Alumina	101.96	-	-	Al_2O_3

Table 2. Properties of chemical used in Silicon dioxide synthesis

Components	**Molecular weight (g/mol)**	**Density (g/ml)**	**Purity**	**Formula**
Ethanol	46.07	0.79	0.995	EtOH
Water	18.02	0.999	1	H_2O
Hydrochloric Acid	36.45	1.17	0.37	HCl
TEOS	208.33	0.934	0.98	$Si(OC_2H_5)_4$

In the synthesis of the Ni/ZnO-TiO_2 catalysts, tetrabutyl orthotitanate (TBOT) was the precursor for titanium dioxide and zinc nitrate hexahydrate ($Zn(NO_3)_2.6H_2O$) was precursor for zinc oxide source. Ethanol (EtOH) and deionized water (DIW) were used as solvents. Hydrochloric acid (HCl) was used as peptizing agent. Ni precursor was Ni(II) acetate. Properties of chemicals are given in Table 3.

Table 3. Properties of chemicals used in Ni/ZnO-TiO_2 mixed oxide catalyst

Components	Molecular weight /g/mol)	Density(g/ml)	Purity %
TBOT	340.36	1	97
H_2O	18	0.998	100
HCl	36.45	1.17	37
EtOH	46.07	0.79	99.5
$Zn(NO_3)_2.6H_2O$	297.48	-	98

3.2. Methods

In this study, the experiments can be categorized into five groups: catalyst preparation, catalyst characterization, starch hydrolysis, product characterization, experimental designs.

3.2.1. Catalyst preparation

Ni/SiO_2-Al_2O_3 catalysts were synthesized using modified sol gel methods developed in Prof.Dr. Erol Seker's research group. To prepare silica sol; first, a necessary amount of TEOS, ethanol (EtOH), HCl, H_2O (distilled water) were mixed at 85°C for 1 h. To prepare alumina sol; first, necessary amount of aluminum isopropoxide (AIP), water, and H_2SO_4 were mixed at 85°C for 1 h. Then, Nickel II acetate was added to prepared alumina sol and was mixed for 10 minutes. After that, the previously prepared silica sol was added to Nickel II acetate mixed alumina sol. The final mixed sol was stirred at the same temperature for 3 h. Then, excess water was evaporated to obtain mixed oxide gel. All the gels were dried at 120 ^oC for 18 h and the dried catalysts were calcined at a temperature mentioned before for 6 h. Finally, all the calcined catalysts were ground to mesh sizes less than 75 μm.

Ni/ZnO-TiO_2 catalysts were synthesized using modified sol gel methods developed in Prof.Dr. Erol Seker's research group. To prepare mixed sol, TBOT and ethanol were mixed in a glove box. A necessary amount of H_2O (distilled water) and HCl were mixed at room temperature. Then, a necessary amount of H_2O (distilled water), zinc nitrate hexahydrate (Zn $(NO_3)_2.6H_2O$) were mixed in a separate beaker at room temperature. After that, the mixtures were added to TBOT and ethanol mixture. The final mixture was stirred until the gel was formed. All the gels were dried at 120 ^oC for 24 h. Then, the dried catalysts were calcined at a specified temperature for 6 h. Finally, all the calcined catalysts were ground to mesh sizes less than 75 μm. The schematics for sol gel procedures used for Ni/SiO_2-Al_2O_3 and Ni/ZnO-TiO_2 catalysts were given in Figure 5 and 6.

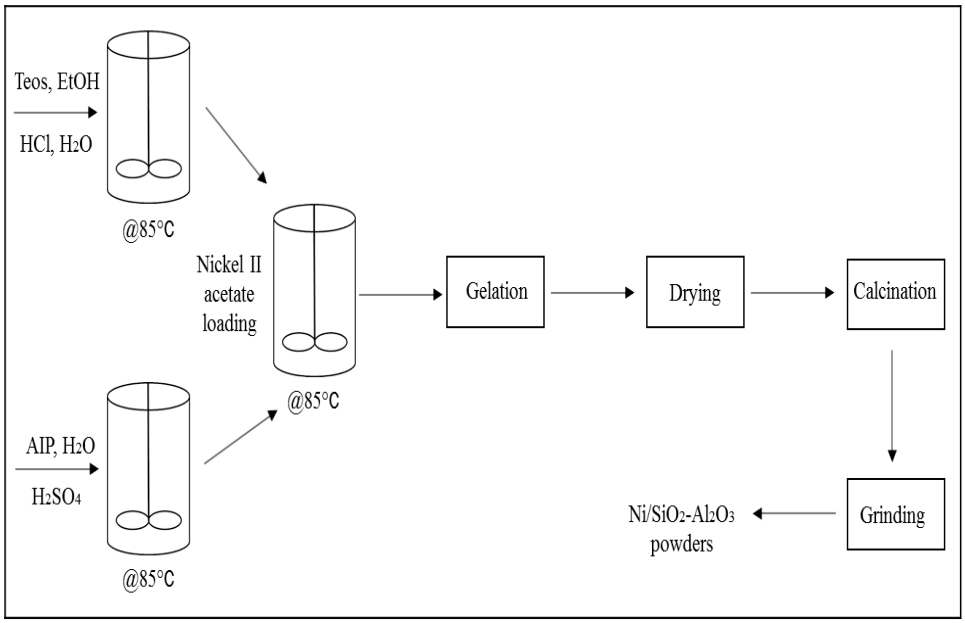

Figure 5. Experimental procedure to synthesize Ni doped SiO_2-Al_2O_3 catalysts.

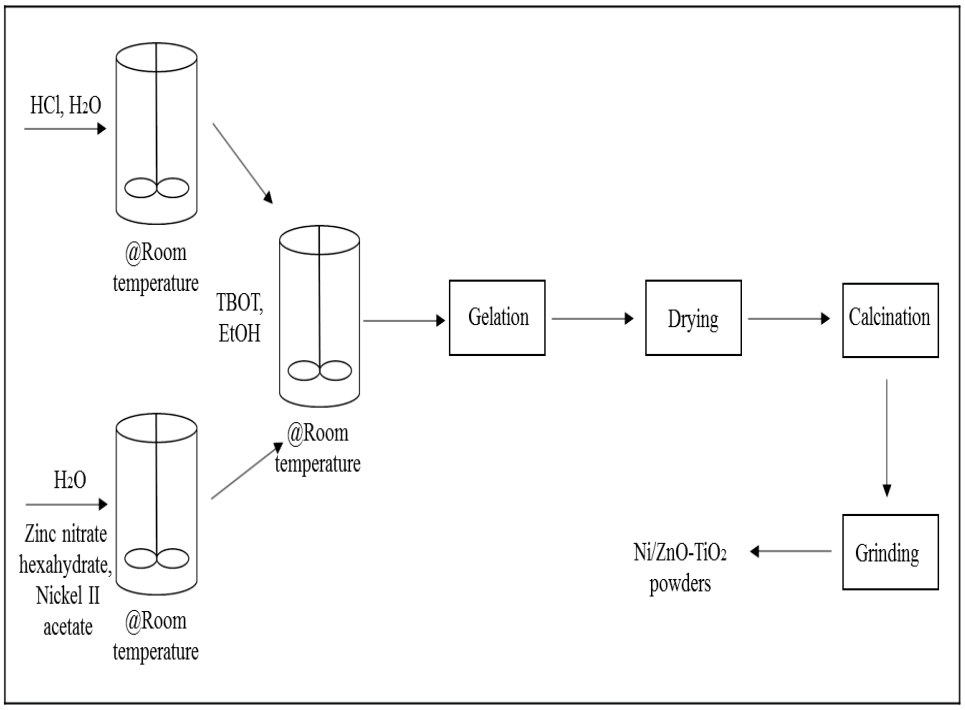

Figure 6. Experimental procedure to synthesize Ni doped ZnO-TiO_2 catalysts.

3.2.2. Catalyst characterization

The physicochemical properties of the catalysts were determined using NH_3-TPD and X-Ray Diffraction (XRD).

3.2.2.1. NH_3-Temperature Programmed Desorption (NH_3-TPD)

A description of acidic properties of a solid surface requires the determination of acidity (i.e. acid amount), the acidic strength and the nature (e.g. Bronsted or Lewis type) of the acidic sites. The amount of acid on a solid, called acidity, is expressed as the number of moles of acid sites per unit amount of catalyst or per unit surface area of the solid catalyst. Acidity is generated on the solid catalyst by an excess of a negative or positive charge in the structure of binary oxides, such as SiO_2-Al_2O_3, ZnO-TiO_2 (Tanabe et al., 1989). The acidity depends on compositions of catalysts (For example: Si/Al ratio) (Hattori and Ono, 2015) and calcination temperatures (Tanabe et a., 1989).

The acid strength of a solid is defined as the ability of the surface to convert an adsorbed neutral base into its conjugate acid. The acid strength of a solid depends on compositions of catalysts and calcination temperatures, too (Tanabe et a., 1989).

The amount and strength of acid sites could be measured using NH_3- TPD. However, the nature of acid sites (i.e. Bronsted or Lewis) could not be determined with TPD technique. In this method, ammonia molecules adsorbed on all the acid sites were desorbed into inert gas, such as helium, as the temperature was increased at a heating rate. The emerging of NH_3, detected by the chemisorption instrument as temperature increased, was recorded as a function of temperature. The total area under the peaks gave the total acidity of the catalyst while the location of the peaks, i.e. the temperature of the desorbing NH_3, gave the acidic strength of the catalyst. The higher the desorption temperature, the higher the acidic strength. It is possible to observe more than one peak in NH_3-TPD; thus, indicating the varying acidic strengths on the solid catalyst.

3.2.2.2. X-Ray Diffraction (XRD)

The crystalline phases and the crystallite sizes were determined using X-Ray Diffraction (XRD). XRD spectra of the catalysts were measured using Philips X'Pert Pro X-ray diffractometer operated at 40 kV and 45 mA. The average crystallite sizes were calculated using the peak broadening of the diffraction peaks and Scherrer equation.

3.2.3. Starch Hydrolysis

Starch (0.4 g) was dissolved in H_2O (100 mL). The resulting mixture was sonicated at 80 ^oC for 45 min. Then, the mixture was heated and stirred at 90 ^oC for 1 h. Then, the solution was passed through a filter (7-12 μm). After that, the catalyst (0.6 g) was added to filtered starch solution (15 ml). The reaction was carried out at 90 ^0C for 24 h. The schematic of starch hydrolysis carried out on the catalyst surface is shown in Figure 7.

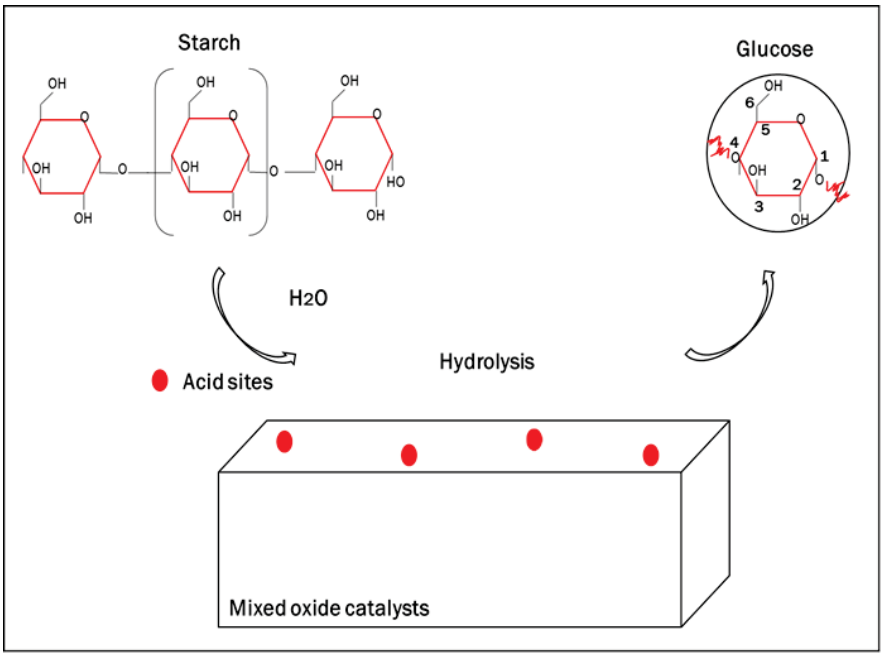

Figure 7. Starch hydrolysis with the aid of mixed oxide catalysts

3.2.4. Products Analyses

The starch hydrolysis products were analyzed using High Performance Liquid Chromatography (HPLC) and also, dissolved metals, such as Ni, were determined using Inductively Coupled Plasma- Mass Spectrometer (ICP-MS).

3.2.4.1. High Performance Liquid Chromatography (HPLC) Analysis

Agilent 1100 High performance liquid chromatography (HPLC) equipped with refractive index detector was used to measure the amounts of products after starch hydrolysis reaction. Thermo Fisher Scientific HyperREZ XP Carbohydrate H+ 8 µm column was used to separate the saccharide products and the refractive index detector quantified the separated products eluding from the column. The mobile phase was ultrapure water. The column was operated at 65 ^{o}C.

3.2.4.2. Inductively Coupled Plasma-Mass Spectrometer (ICP-MS)

The amount of nickel loss from prepared Ni doped SiO_2-Al_2O_3 was measured using ICP-MS Agilent 7500 ce.

3.2.5. Experimental Design

To find the effect of the reaction conditions on the product distribution, Box-Behnken experiment design was carried out for two types of mixed oxide catalysts.

3.2.5.1. Box-Behnken experimental design for Ni/SiO_2-Al_2O_3 catalysts

There were 3 factors, 1 replicates, 1 total blocks, 3 center points. Total runs of experiments were 15. Compositions were varied from 30 wt.% to 70 wt.% for SiO_2-Al_2O_3, Ni loading was varied from 1 wt.% to 10 wt.% and the calcination temperatures were changed from 500 ^oC to 900 ^oC with a 200 ^oC of increment. Box- Behnken experimental design for Ni/SiO_2-Al_2O_3 catalyst was given in Table 4

Table 4. Box-Behnken experimental design for Ni/SiO_2-Al_2O_3

Experimental Run Number	Composition (SiO_2-Al_2O_3)	Ni % Loading	Calcination Temperature (°C)
1	30/70	1	700
2	70/30	1	700
3	30/70	10	700
4	70/30	10	700
5	30/70	5.5	500
6	70/30	5.5	500
7	30/70	5.5	900
8	70/30	5.5	900
9	50/50	1	500
10	50/50	10	500
11	50/50	1	900
12	50/50	10	900
13	50/50	5.5	700
14	50/50	5.5	700
15	50/50	5.5	700

3.2.5.2. Box-Behnken experimental design for Ni/ZnO-TiO_2 catalysts

There were 3 factors, 1 replicates, 1 total blocks, 3 center points. Total runs of experiments were 15. Compositions were varied from 10 wt.% to 90 wt.% for ZnO-TiO_2, Ni loading was changed from 1 wt.% to 10 wt.% and the calcination temperatures were increased from 300 ^{0}C to 500 ^{0}C with a 200 ^{o}C of increment. Box- Behnken experimental design for Ni/ZnO-TiO_2 catalyst was given in Table 5.

Table 5. Box-Behnken experimental design for Ni/ZnO-TiO_2

Experimental Run Number	**Composition (ZnO-TiO_2)**	**Ni % Loading**	**Calcination Temperature (°C)**
1	10/90	1	400
2	50/50	1	400
3	10/90	10	400
4	50/50	10	400
5	10/90	5.5	300
6	50/50	5.5	300
7	10/90	5.5	500
8	50/50	5.5	500
9	30/70	1	300
10	30/70	10	300
11	30/70	1	500
12	30/70	10	500
13	30/70	5.5	400
14	30/70	5.5	400
15	30/70	5.5	400

CHAPTER 4

RESULTS AND DISCUSSION

4.1. Characterization of Starch Hydrolysis Products

In this study, starch hydrolysis products were analyzed using HPLC. The operating conditions of HyperREZ XP Carbohydrate H^+ column given the literature was 75 ^oC, 0.6 mL/min with mobile phase ultrapure water. Under such operating condition, the retention times of common saccharides were known as 9.9 min for glucose, 8.4 min for maltose, 7.7 min for maltotriose, 10.6 min for xylose. In this study, the operating condition of the column was slightly different: 65 ^oC, 0.38 mL/min with mobile phase ultrapure water. Thus, the retention times for all the saccharides shifted to higher times; for instance,at 15.32 min, glucose eluded (it was confirmed using glucose standard) and also 14. min for maltose standard at this operating condition. The chromatogram of glucose (100 ppm) and maltose (100 ppm) standards were given in Appendix A. The retention times were given in Table 6 They were changed 5.5 ± 0.1 minutes at 65 ^oC, 0.38 mL/min. The HPLC chromatogram for retention times of products and calibration curve of glucose were given in Appendix A.

Table 6. Retention times for starch hydrolysis products

Compound	**Retention Time (min)**
Glucose	15.3
Xylose	16.3
Maltotriose	13.1
Unknown saccharides	-

The concentration of the glucose was calculated based on calibration curve of glucose standard. It is known that for saccharide concentration less than 1 wt.%, the refractive index does not change with the type of the saccharide but with the concentration. In fact, it was also confirmed in this study when glucose (100 ppm) and

maltose (100 ppm) standards were used, both standards gave the same area under curve in the HPLC equipped with the refractive index. Thus, the amounts of all the saccharides with concentration less than 1 wt.%, observed in HPLC, were determined using glucose calibration curve. Unfortunately, for the amounts larger than 1 wt.% of known and unknown saccharides, the area percentages were utilized to report the product distribution. The general expression of a species yield % was calculated as shown below

$$Species\ yield\% = \frac{Amount\ of species\ (g) in\ product distribution}{Initial\ Amount\ of\ starch\ (g)} * 100 \qquad (4.1)$$

The carbon balance for all the reaction could not be closed because of two reasons: 1) the number n in the starch molecule $(C_6H_{10}O_5)_n$ is un known; 2) there are unknown saccharides detected using HPLC. Therefore, starch conversion could not be calculated.

4.2. Determination of Product Distribution for Ni/SiO_2-Al_2O_3 Catalysts

On all the catalysts, glucose, xylose, maltotriose and an unidentifiable saccharide were detected using HPLC, the area percentages of all the products were given in Table 8 in Appendix A. Since there was an unknown compound with a very large amount, the product concentrations (mg/L) were only given for the species, glucose, xylose and maltotriose, in Table 9 in Appendix A. Using the concentrations given in Table 9, glucose yield % was ploted in Figure 8.

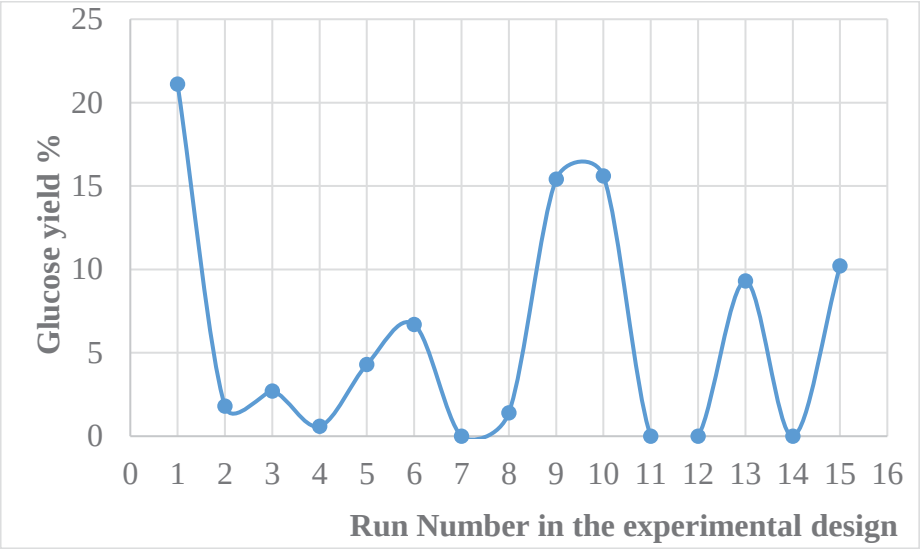

Figure 8. Glucose yield % for Ni/SiO_2-Al_2O_3 catalysts

As seen in the Figure 8, 1%Ni/ 30% SiO_2-70% Al_2O_3 (run number 1) catalyst, that was calcined at 700 ^oC for 6 h, gave the highest glucose yield% of 21.1%. The corresponding HPLC chromatogram of the products obtained on 1%Ni/ 30% SiO_2-70% Al_2O_3 catalyst was given in Appendix A. The second highest glucose yield %, ~15.4%, was observed on 1%Ni/ 50% SiO_2- 50% Al_2O_3 (run number 9) catalyst that was calcined at 500 ^oC for 6 h and also on 10%Ni/ 50% SiO_2- 50% Al_2O_3 (run number 10) catalyst that was calcined at 500 ^oC for 6 h. In contrast to these catalysts, 1% Ni / 50% SiO_2- 50% Al_2O_3 (run number 11) catalyst that was calcined at 900 ^oC for 6 h and 10% Ni / 50% SiO_2- 50% Al_2O_3 (run number 12) catalyst that calcined at 900 ^oC for 6 h gave no glucose yield within the experimental uncertainty, ±9%, of this study.

4.3. Determination of Products for Ni/ZnO-TiO_2 Catalysts

On all the catalysts, glucose and an unidentifiable saccharide were detected using HPLC. The area percentages of all the products were given in Table 10 in Appendix A. Unknown saccharide yield was ~100% on all of the catalysts. The chromatogram for 10%Ni/ 10% ZnO-90% TiO_2 catalyst that was calcined at 400 ^0C for 6 h was given in Figure 9. As seen in the figure, there was only one peak corresponding to an unknown saccharide. It was found that regardless of ZnO wt.%-TiO_2 wt.% and also Ni wt.%, there was only one unknown compound detected using HPLC. Although glucose was observed on some catalysts, such as 10%Ni/10%ZnO-90%TiO2 or 5.5%Ni/30%ZnO-70%TiO2

which were calcined at 400 ^{o}C, the concentration of the glucose was found to be less than 25 mg/L, which was very low as compared to the initial concentration of starch (40000 mg/L).

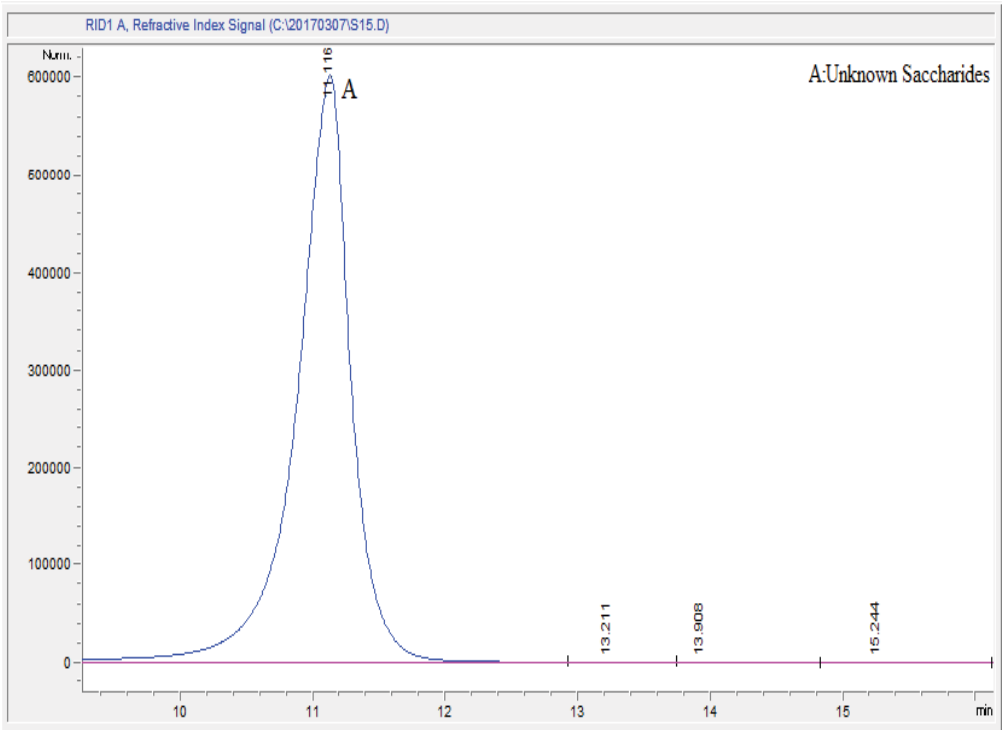

Figure 9. HPLC chromatogram for 10%Ni/ 10%ZnO-90% TiO_2

4.4. Determination of Nickel Loss Amount from Prepared Ni/SiO_2-Al_2O_3

The amount of Nickel (Ni) lost from Ni/ SiO_2-Al_2O_3 catalysts were determined using ICP-MS. For 5.5% Ni/ 30% SiO_2-70% Al_2O_3 catalyst which was calcined at 500 ^{o}C for 6 h, Ni lost during 24 h of starch hydrolysis at 90 ^{o}C was found to be 337.2 mg/L. In contrast, Ni loss decreased to 25.2 mg/L for 5.5% Ni/ 50%SiO_2 – 50% Al_2O_3 which was calcined at 700 ^{o}C for 6 h and Ni loss was found to decrease to 1.41 mg/L for 5.5% Ni/ 70% SiO_2- 30% Al_2O_3 which was calcined at 900 ^{o}C for 6 h. These showed that Ni loss strongly depended on the amount of SiO_2 content and also the calcination temperature. In other words, higher the SiO_2 and calcination temperature, the lower the Ni loss.

4.5. The Effect of Crystallite Size and Phase of Catalysts

The effect of crystallite size and crystalline phases of all the catalysts were investigated using high angle XRD. The crystallite size was calculated using Scherrer equation shown in the equation 3 below:

$$D = \frac{K*\lambda}{B*cos\theta} \quad (4.2)$$

Where D was the crystal size, K was the Scherrer constant which is usually 0.94, λ was the wavelength of the X-ray, B was the broadening of a diffraction peak, found using the full width at half maximum and given in 2θ radian, and θ was the diffraction angle of the same peak (Patterson 1939).

XRD patterns of 1%Ni/ 70% SiO_2-30% Al_2O_3 (run number 2) catalyst that calcined at 700 ^oC for 6 h that gave 1.8% glucose yield. The catalyst showed $Al_2(SO_4)_3$ diffraction peaks as seen in Figure 10. The crystallite size of $Al_2(SO_4)_3$ was calculated to be 23 nm. However, nickel peaks could not be detected on all the catalysts since XRD was insensitive to crystallite sizes less than 5 nm. In other words, Ni crystallite size on all ythe catalysts was less than 5 nm.

XRD patterns of 10%Ni/ 50% SiO_2- 50% Al_2O_3 (run number 10) catalyst that calcined at 500 ^oC for 6 h gave 15.6% glucose yield. The major diffraction peaks were found to be that of $Al_2(SO_4)_3$ crystalline phase as given in Figure 11. The crystallite size of $Al_2(SO_4)_3$ was calculated to be 42 nm.

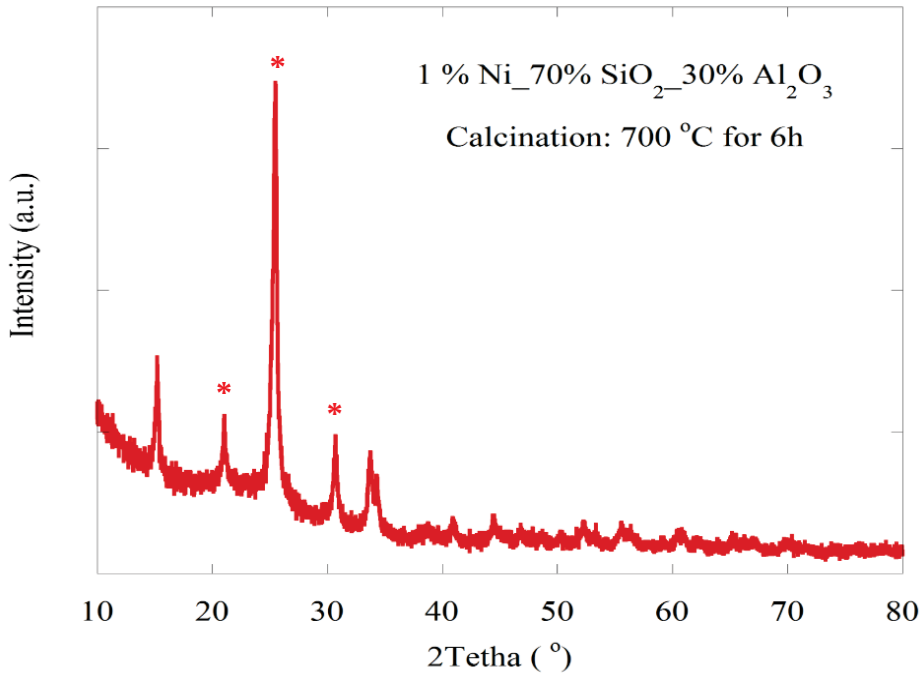

Figure 10. X-Ray Intensity versus 2θ angle values of 1% Ni/ 70% SiO_2- 30% Al_2O_3 catalyst calcined at 700 ºC for 6 h.

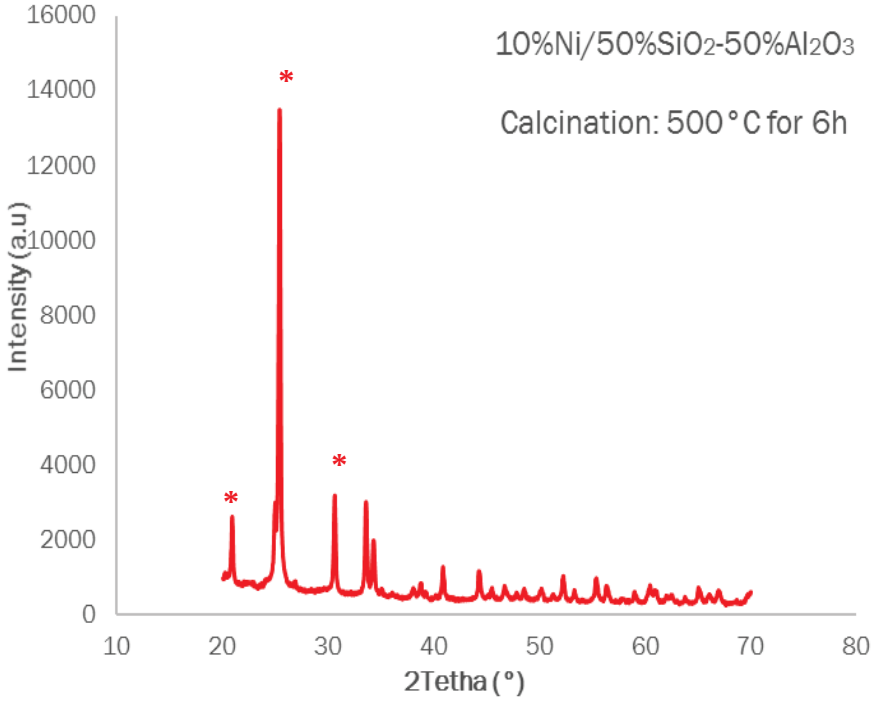

Figure 11. X-Ray Intensity versus 2θ angle values of 10% Ni/ 50% SiO_2- 50% Al_2O_3 catalyst calcined at 500 ºC for 6 h.

XRD patterns for 10%Ni/ 50% SiO_2- 50% Al_2O_3 (run number 12) catalyst that calcined at 900 ^oC for 6 h was given in Figure 12. On this catalyst, the glucose yield was found to be 0%. The major XRD peaks corresponded to $Al_2(SO_4)_3$crystaline phase. The crystallite size of $Al_2(SO_4)_3$ was calculated to be 10.5 nm.

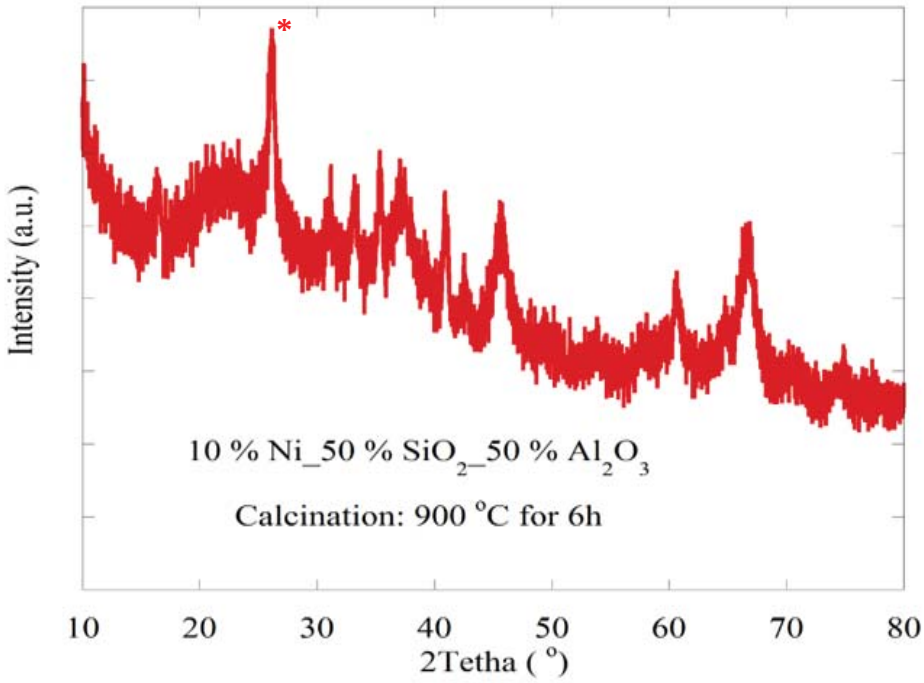

Figure 12. X-Ray Intensity versus 2θ angle values of 10% Ni/ 50% SiO_2- 50% Al_2O_3 catalyst calcined at 900 ^oC for 6 h.

XRD patterns given Figure 11. and Figure12. showed that the crystallite size of $Al_2(SO_4)_3$ was dependent on the calcination temperature. As the calcination temperature was increased from 500 ^{o} to 900 ^oC for the same catalyst composition, the crystallite size of $Al_2(SO_4)_3$ decreased from 42 to 10.5 nm. This seemed to indicate that the smaller the $Al_2(SO_4)_3$ crystallite size, the lower the glucose yield. In other words, starch hydrolysis seemed to selectively proceed to glucose on large $Al_2(SO_4)_3$ crystallite size; thus, the starch hydrolysis reaction is the structure sensitive reaction.

XRD patterns of 10%Ni/ 30%ZnO- 70% TiO_2 (run number 10) catalyst that calcined at 300 ^oC for 6 h was given in Figure 13. The catalyst showed TiO_2 diffraction peaks corresponding to anatase crystalline phase. TiO_2 anatase crystallite size was 8.6 nm. ZnO and nickel peaks was not observed on all the catalysts since XRD was insensitive to crystallite sizes less than 5 nm; hence this showed that the crystallite size for Ni and ZnO crystalline phases was less than 5 nm. Glucose yield on all the catalysts was almost zero regardless of catalyst composition and the calcination temperatures.

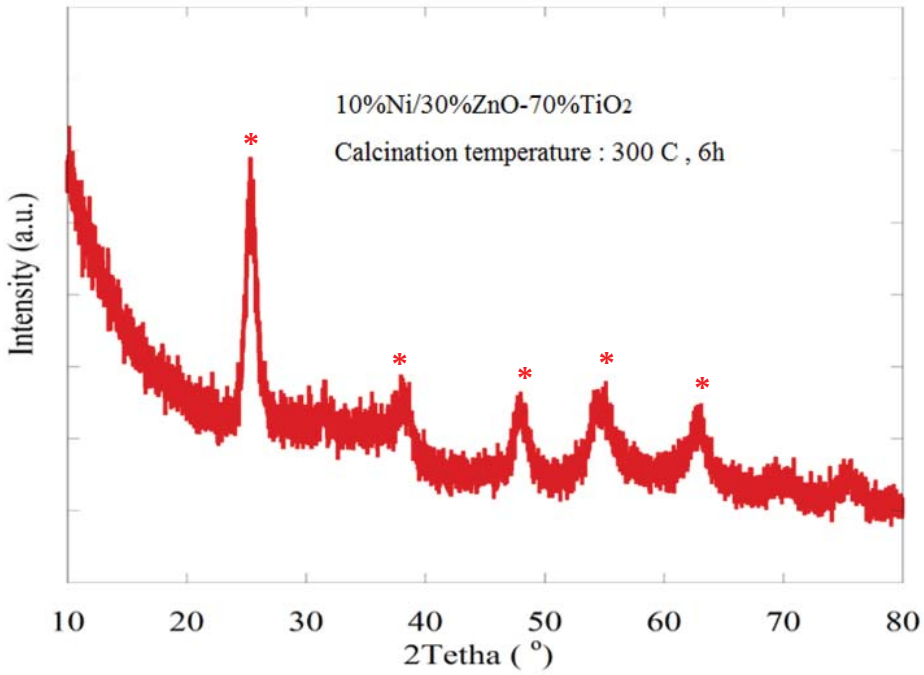

Figure 13. X-Ray Intensity versus 2θ angle values of 10% Ni/ 30% ZnO-70% TiO_2 catalyst calcined at 300 °C for 6 h.

4.6. The Effect of Acidity and Acidic Strength of Catalysts

It is well known that the hydrolysis of starch is accelerated when acid catalysts is used. SiO_2-Al_2O_3 and ZnO-TiO_2 were reported to be mixed oxide solid acid catalysts (Tanabe 1989). The acidity and acidic strength of the selected catalysts were determined using NH_3-TPD to clarify the reason behind the variation in product distribution observed during the hydrolysis of starch. To determine the total acidity of the catalysts, NH_3 was used as a probe molecule. When the NH_3 molecule was held strongly on the surface, it was desorbed at higher temperatures; thus, indicating the acidic strength of the catalyst.

NH_3-TPD of 1%Ni/ 50% SiO_2- 50% Al_2O_3 (run number 9) catalyst that calcined at 500 °C for 6 h was given in Figure 14. It was found that there were two NH_3 desorption temperatures, 156 °C and 316 °C, as seen in Figure 14. The total acidity, corresponding to the total area under the curve, was found to be 2.96 µmol/g of the catalyst. In fact, the glucose yield on the catalyst was 15.4%. However, the glucose yield was 15.6% on 10%Ni/ 50% SiO_2- 50% Al_2O_3 (run number 10) catalyst that calcined at 500 °C for 6 h. In fact, within the experimental uncertainty of the study, the glucose yield was the same as that observed on 1%Ni/ 50% SiO_2- 50% Al_2O_3. NH_3-TPD of 10%Ni/ 50% SiO_2- 50% Al_2O_3 was given in Figure 16. It was found that there were two desorption temperatures

located at 163 ^{o}C and 423 ^{o}C. The total acidity of 10%Ni/ 50% SiO_2- 50% Al_2O_3 was found to be 4.69 μmol/g of the catalyst. One may expect to obtain higher glucose yield on the catalyst composition having higher total acidity since the hydrolysis reaction occurred faster on more acidic condition. However, it was found that not only the acidity but also acidic strength important. It seems that the both catalysts had the same NH_3 desorption peak located at 156 ^{o}C that seemed to be responsible for starch hydrolysis as opposed to the NH_3 desorption peaks located at higher temperatures, such as 316 ^{o}C and 423 ^{o}C.

NH_3-TPD of 10%Ni/ 30% SiO_2- 70% Al_2O_3 (run number 4) catalyst that calcined at 700 ^{o}C for 6 h was given in Figure 15. It was found that there was one NH_3 desorption temperature located at ~200 ^{o}C as seen in Figure 15. The total acidity of the catalyst was found to be 1.1 μmol/g of the catalyst. The glucose yield was 2.7% on this catalyst. In fact, it seemed thatthe slightly higher acidic strength but 4 times less acidity observed on 10%Ni/ 30% SiO_2- 70% Al_2O_3 catalyst was responsible for much lower glucose yield, 2.7%, as compared to the higher glucose yield, 15.4%, obtained on 1%Ni/ 50% SiO_2- 50% Al_2O_3 and 10%Ni/ 50% SiO_2- 50% Al_2O_3 catalysts. In other words, the acidity is the most important factor in selective production of glucose but the acidic strength must be considered, too.

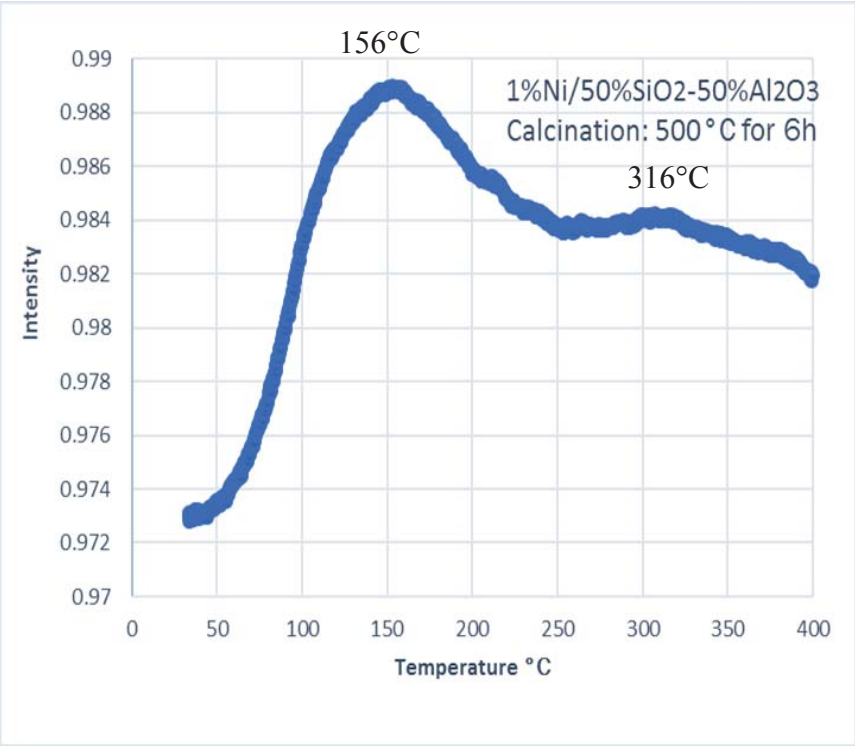

Figure 14. TPD of 1%Ni/50%SiO_2-50%Al_2O_3 catalyst calcined at 500 °C for 6 h

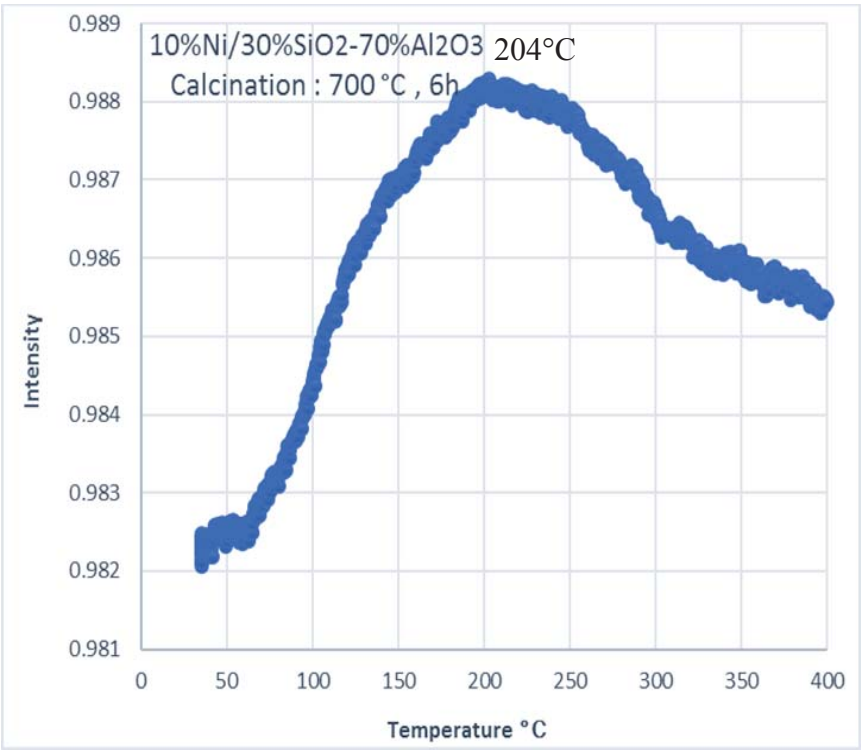

Figure 15. TPD of 10% Ni/30% SiO_2-70% Al_2O_3 catalyst calcined at 700 °C for 6 h

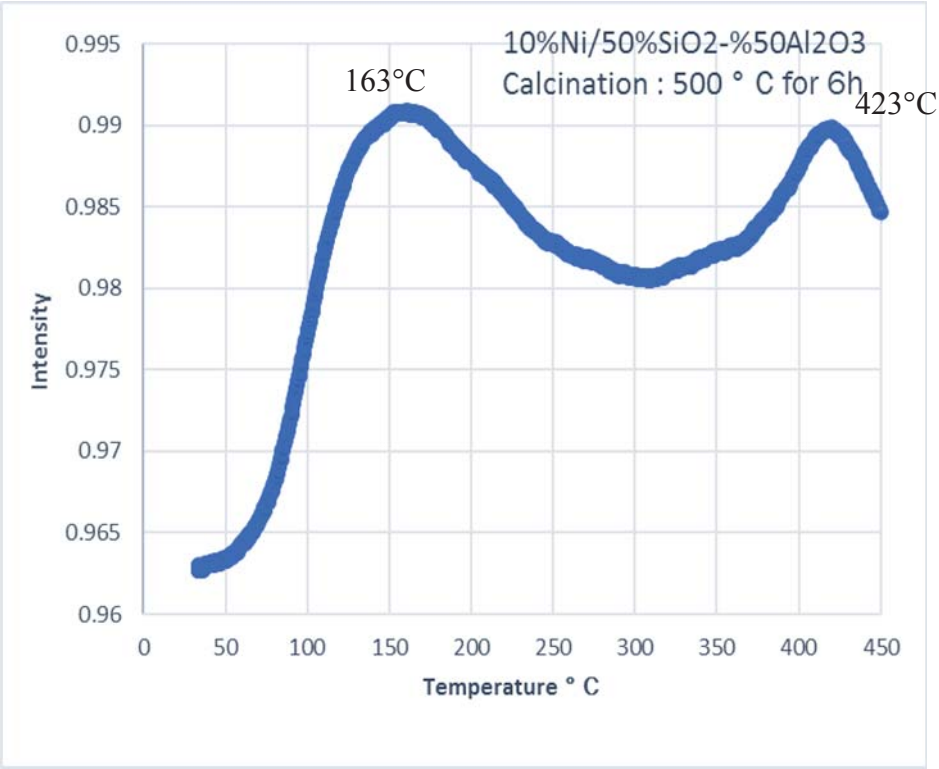

Figure 16. TPD of 10%Ni/50%SiO_2-50%Al_2O_3 catalyst calcined at 500 °C for 6 h

NH_3-TPD of 10%Ni/ 50% SiO_2- 50% Al_2O_3 (run number 12) catalyst that calcined at 900 ^oC for 6 h was given in Figure 17. It was found that there seemed to be two NH_3 desorption temperatures located at 148 ^oC and 256 ^oC as seen in Figure 17. The total acidity of the catalyst was found to be 1.69 µmol/g of the catalyst. The glucose yield on this catalyst was 0.0 %. Even though the total acidity was similar to that observed on 10%Ni/ 30% SiO_2- 70% Al_2O_3 (run number 4) catalyst that calcined at 700 ^oC for 6 h, the acidic strength of 10%Ni/ 50% SiO_2- 50% Al_2O_3 catalyst was also slightly lower than that 10%Ni/ 30% SiO_2- 70% Al_2O_3 catalyst. Besides, it was found that the crystallite size of $Al_2(SO_4)_3$ crystalline phase on 10%Ni/ 50% SiO_2- 50% Al_2O_3 (run number 12) catalyst that calcined at 900 ^oC for 6 h was ~4 times smaller than that of 10%Ni/ 50% SiO_2- 50% Al_2O_3 (run number 10) catalyst that calcined at 500 ^oC for 6 h. Thus, it was found that crystallite size of $Al_2(SO_4)_3$ crystalline phase must be large in addition to having the high acidity and low acidic strength centered at ~150 ^oC in order to have high glucose yields.

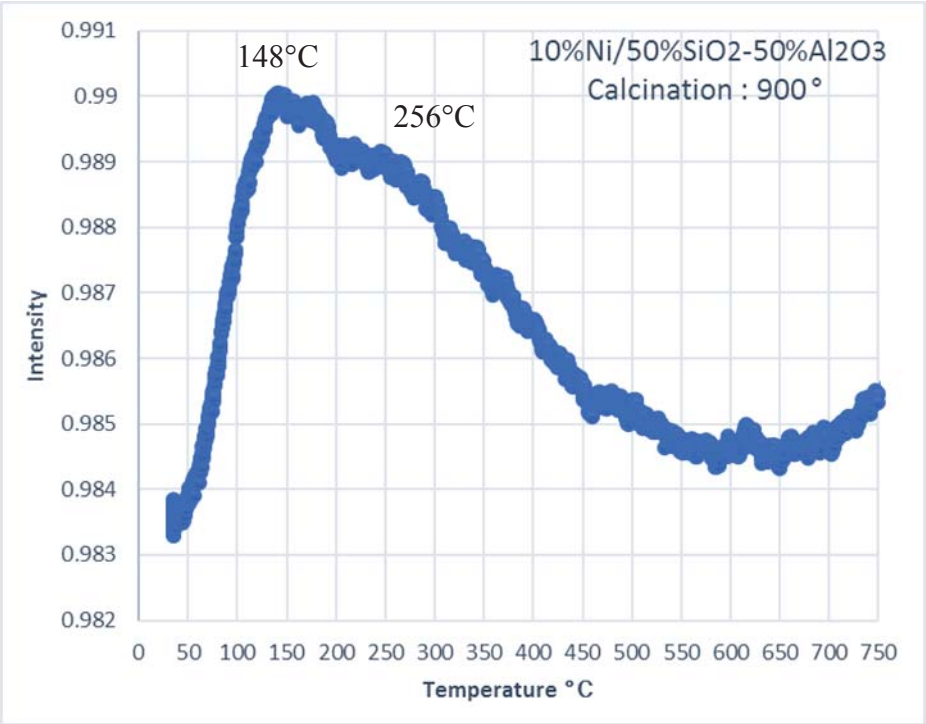

Figure 17. TPD of 10%Ni/50%SiO_2-50%Al_2O_3 catalyst calcined at 900 °C for 6 h

NH_3-TPD of 10% Ni/ 10% ZnO-90% TiO_2 catalyst that calcined at 400 ^{0}C for 6 h was given in Figure 18. It was found that there was one NH_3 desorption temperature located at 200 ^{o}C and the total acidity was found to be 3.78 µmol/g of the catalyst as seen in Figure 18. The glucose yield on this catalyst was 0.0 %. This showed that not only acidity and acidic strength was important but also acid type was more important. It means that the acid type on $Al_2(SO_4)_3$ crystalline phase was more active than the acid type on ZnO and TiO_2 anatase crystalline phases. Similarly, NH_3-TPD of 10% Ni/ 50% ZnO-50% TiO_2 catalyst that calcined at 400 ^{0}C for 6 h was given in Figure 4.19. It was found that there was one NH_3 desorption temperature located at 204 ^{o}C and the total acidity was 4.69 µmol/g of the catalyst. On this catalyst, the glucose yield was 0.0 %, too. This also showed that not only acidity and acidic strength was important but also acid type was more important.

Upon the results found in this study, it is recommended that the detailed analyses on the acid type must be investigated using in situ FTIR and a controlled dosage of a probe molecule.

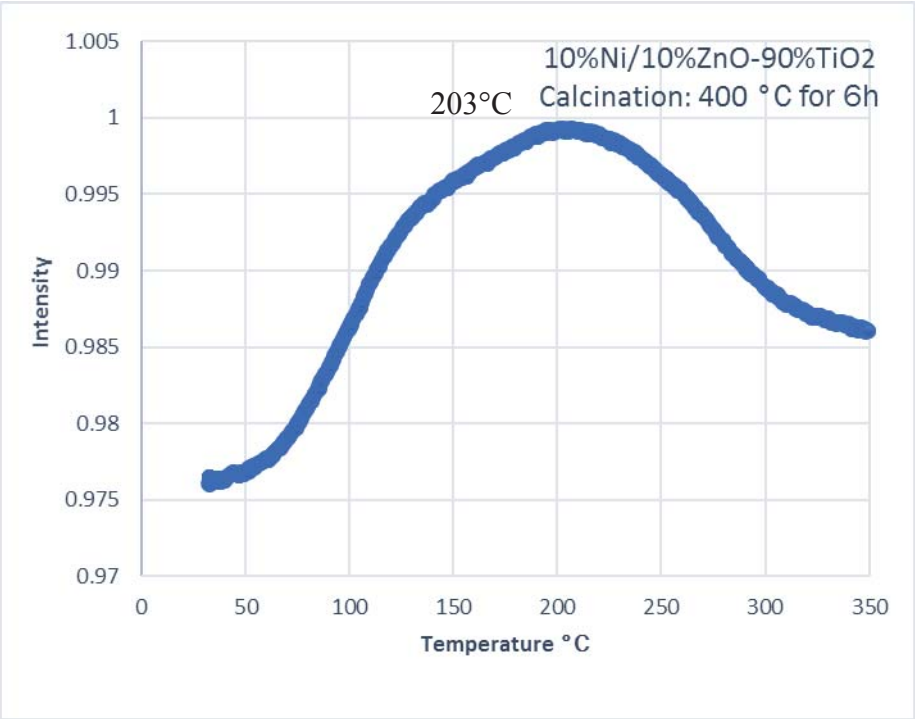

Figure 18. TPD of 10%Ni/10%ZnO-90%TiO_2 catalyst calcined at 400 ºC for 6 h

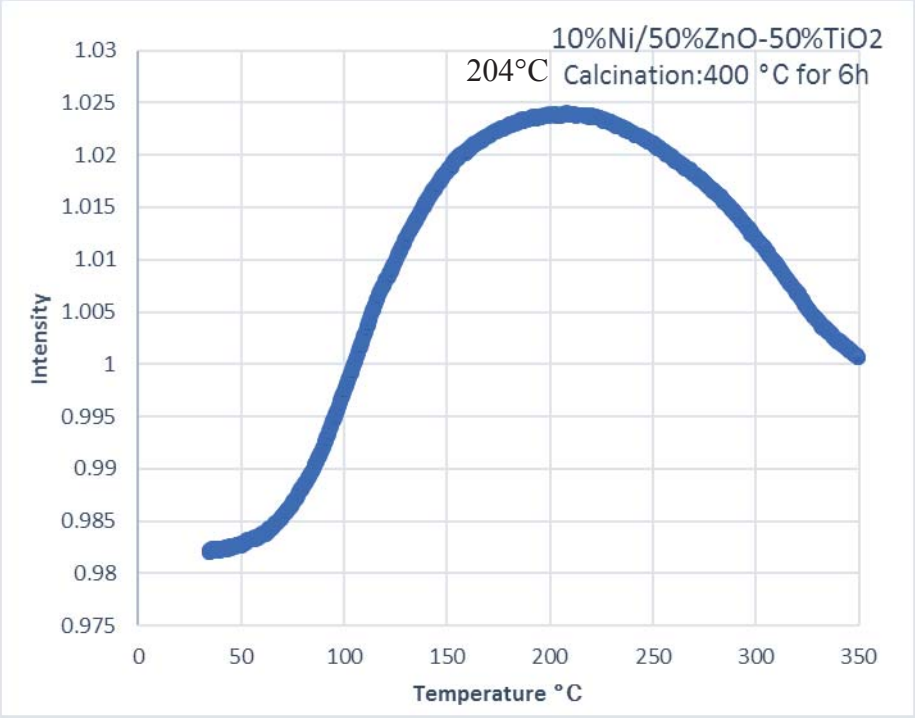

Figure 19. TPD of 10%Ni/50%ZnO-50%TiO_2 catalyst calcined at 400 ºC for 6 h

CHAPTER 5

CONCLUSION

In this study, the effects of acidity (amount of the acidic sites) and acid strength of the mixed oxide supported Ni catalysts and/or the crystalline phase and crystallite size on the product distribution during starch hydrolysis were investigated at 90 ^{o}C and 24 h of reaction time.

The major outcome of this study can be summarized as follows:

- On all the Ni/SiO_2-Al_2O_3 catalysts, glucose, xylose, maltotriose and an unidentifiable saccharide were observed. A maximum glucose yield of 21% was obtained on 1%Ni/ 30% SiO_2-70% Al_2O_3 (run number 1) catalyst, that was calcined at 700 ^{o}C for 6 h.
- On all the Ni/ZnO-TiO_2 catalysts, a small amount of glucose, less than 25 mg/L, and a large amount of unidentifiable saccharide were observed regardless of the catalyst composition and the calcination temperatures.
- The product distribution was affected by the nature of the acid type; for instance, $Al_2(SO_4)_3$ crystalline phase was more active than the acid type on ZnO and TiO_2 anatase crystalline phases.
- The larger $Al_2(SO_4)_3$ crystallite sizes, e.g. 42 nm, increased the glucose yield.

Acidic strength was more important than total acidity for the same acid type. In fact, the lower the acidic strength higher the glucose yield was obtained.

REFERENCES

Babu, Vikash, Thapliyal, Ashish, and Girijesh Kumar Patel. Biofuels Production, Beverly: Scrivener Publishing, 2014.

Balat M. and Balat H., Recent trend in global production and utilization of bio-ethanol fuel, Applied Energy, 86 (2009), 2273-2282.

BeMiller, James, and Roy Whistler. Starch: Chemistry and Technology. USA: Elsevier, 2009.

Cauqui M.A., Izquierdo J.M.R., Application of the sol-gel methods to catalyst preparation, Journal of Non-Crystalline Solids, 147&148 (1992), 724-738.

Burck J., Marten F., Bals C., Dertinger A., Uhlich T., Climate Change Performance Index, (2017).

Chambre D., Szabo M.R., Popescu C., Iditoiu C., Heterogeneous soft and acid catalysis of the sucrose hydrolysis, Journal of Thermal Analysis and Calorimetry, Volume 94, (2008), 417-420.

Cheng M., Shi T., Guan H., Wang S., Wang X., Jiang Z., Clean production of glucose from polysaccharides using a micellar heteropolyacid as a heterogeneous catalyst, Applied Catalysis B: Environmental, Volume 107, Issue 1-2, (2011), 104-109.

Choi J.H., Kim S.B., Effect of ultrasound on sulfuric acid-catalyzed hydrolysis of starch, Korean Journal of Chemical Engineering, Volume 11, Issue 3, (1994), 178-184.

Choi H.W., Lee J.H., Ahn S.C., Kim B.Y., Baik M.Y., Effects of ultrahigh pressure, pressing time and HCl concentration on non-thermal starch hydrolysis using ultra high pressure, Starch, Volume 61, Issue 6, (2009), 334-343.

Dhepe P.L., Ohashi M., Inagaki S., Ichikawa M, Fukuoka A., Hydrolysis of sugars catalyzed by water-tolerant sulfonated mesoporous silicas, Catalysis Letters, Volume 102, (2005), 3-4.

FAO (2008)., The State of Food And Agriculture, 2008 Edition. Rome, www.fao.org/catalog/inter-e.htm.

Fontana J.D, Mitchell D.A., Molina O.E., Gaitan A., Bonfim T.M.B., Adelmann J., Grzybowski A., Passos M., Starch depolymerization with diluted phosphoric acid and application of the hydrolysate in astaxanthin fermentation, Food Technology Biotechnology, 46 (3) (2008), 305-310.

Gaman, P.M, and K.B. Sherrington, The Science of Food: An Introduction to Food Science Nutrition and Microbiology, Oxford: Pergamon Press, 1981.

Guodong L., Zhengbiao G., Yan H., Caiming L., Structure, functionality and applications of debranched starch: A review, Trends in Food Science & Technology, Volume 63, (2017), 70-79.

Huang Y.B., Fu Y., Hydrolysis of cellulose to glucose by solid acid cataylsts, Green Chemistry, (2013), 1095.

Iloukhani H., Azizian S., Samadani N., Hydrolysis of sucrose by heterogeneous catalysis, Physics and Chemistry of Liquids, Volume 40, Issue 2, (2002), 159-165.

Iwata H., Okada K., Greenhouse gas emissions and the role of the Kyoto Protocol, Environmental Economics and Policy Studies, Volume 16, Issue 4, (2014), 325-342.

Energy Policies of International Energy Agency Countries- Turkey Review, 2016.

International Energy Agency. 2014. World Energy Outlook.

International Energy Agency. 2016. World Energy Outlook.

IPCC, 2014: Climate Change 2014: Mitigation of Climate Change. Contribution of Working Group III to the Fifth Assesment Report of the Intergovernmental Panel on Climate Change [Edenhofer, O., R. Pichs-Madruga, Y.Sokona, E. Farahani, S.Kadner, K.Seyboth, A.Adler, I. Bau, S.Brunner, P.Eickemeier, B Kriemann, J.Savolainen, S. Schlömer, C. von Stechow, T. Zwickel and J.C.Minx (eds)]. Cambridge University Press, Cambridge, United Kingdom and New York, NY, USA.

IRENA (2016), Remap: Roadmap for a Renewable Energy Future, 2016 Edition. International Renewable Energy Agency (IRENA), Abu Dhabi, www.irena.org/remap.

Isıkgor F.H., Becer C.R., Lignocellulosic biomass: a sustainable platform for the production of bio-based chemicals and polymers, Polymer Chemistry, (2015), 6,4497.

Janssen, Leon and Leszek Moscicki. Thermoplastic Starch. Weinheim: Wiley, 2009.

Kapdan I.K., Kargi F., Oztekin R., Effects of operating parameters on acid hydrolysis of ground wheat starch: Maximization of the sugar yield by statistical experiment design, Starch, 63 (2011), 311-318.

Khawla B.J., Sameh M., Imen G., Donyes F., Dhouha G., Roudha E.G., Oumema N.E., Potato peel as feedstock for bioethanol production: A comparison of acidic and enzymatic hydrolysis, Industrial Crops and Products, 52 (2014), 144-149.

Kiran B., Kumar R., Deshmukh D., Perspectives of microalgal biofuels as renewable source of energy, Energy Conversion and Management, 88 (2014), 1228-1244.

Lane, Jim." Biofuels Mandates Around the World:2016." Biofuelsdigest. http://www.biofuelsdigest.com/bdigest/2016/01/03/biofuels-mandates-around-the-world-2016. (accessed January 3, 2016).

Langeroodi N.S., Asghari J., Ghaemi M., Catalytic hydrolysis of sucrose in the presence of vanadium oxide nanoparticles on SiO_2, Russian Chemical Bulletin, Volume 61, Issue 9, (2012), 1822-1824.

Liu G., Gu Z., Hong Y., Cheng L., Li C., Structure, functionality and applications of debranched starch: A review, Trends in Food Science and Technology, 63 (2017), 70-79.

Lorenz K., Johnson J.A., Starch hydrolysis under high temperatures and pressures, Cereal Chemistry, 49 (1972), 616-628.

Marchal L.M., Jonkers J., Franke G.T. Gooijer C.D, Tramper J., The effect of process conditions on the α-amylotic hydrolysis of amylopectin potato starch: An experimental design approach, Biotechnology and Bioengineering, Volume 62 (3), (1998), 348-357.

Mohr S.H., Wang J., Ellem G., Ward J., Giurco D., Projection of world fossil fuels by country, Fuel, 141 (2015), 120-135.

Murthy G.S., Johnston K.D.R., Tumbleson V.S., Starch hydrolysis modeling: application to fuel ethanol production, Bioprocess Biosyst Eng, (2011), 879-890.

Patel A., Gami B., Patel P., Patel B., Microalgae: Antiquity to era of integrated technology, Reneable and Sustainable Energy Reviews, 71 (2017), 535-547.

Perez I.C., Mediavilla M., Castro C., Carpintero O., Miguel L.J., Fossil fuel depletion and socio-economic scenarios: An integrated approach, Energy, Volume 77, (2014), 641-666.

Qi X, Tester R.F., Effect of composition and structure of native starch granules on their susceptibility to hydrolysis by amylase enzymes, Starch, Volume 68, Issue 9-10, (2016), 811-815.

Shafiee S., Topal E., When will fossil fuel reserves be diminished, Energy Policy, 37 (2009) 181-189.

Sheng Xu Q., Yan Y.S., Feng J.X., Efficient hydrolysis of raw starch and ethanol fermentation: a novel raw starch- digesting glucoamylase from Penicillium oxalicum, Biotechnol Biofuels, (2016), 216.

Hattori, Hideshi, and Yoshio Ono. Solis Acid Catalysis From Fundamentals to Applications. Boca Raton: CRC Press, 2015.

Sousa C., Palma C.R., Martins L.F., Economic growth and transport: On the road to sustainability, Natural Resources Forum, 39 (2015), 3-14.

Stoker, Stephen H., Organic and Biological Chemistry, California: Content Technologies, Inc, 2017. netLibrary e-book.

Takagaki A, Tagusagawa C., Domen K., Glucose production from saccharides using layered transition metal oxide and exfoliated nanosheets as a water-tolerant solid acid catalyst, Chemical Communications, 42 (2008), 5363-5365.

Tanabe, Kozo, Misono, Makoto, Ono, Yoshio and Hideshi Hattori. New Solid Acids and Bases Their Catalytic Properties. Tokyo: Elsevier Science, 1989.

Tasic M.B., Konstantinovic B.V., Lazic M.L., Veljkovic V.B., The acid hydrolysis of potato tuber mash in bioethanol production, Biochemical Engineering Journal 43 (2009), 208-211.

Tester R.F., Karkalas J., Qi X., Starch-composition, fine structure and architecture, Journal of Cereal Science, Volume 39, Issue 2, (2004), 151-165.

Tester R.F., Qi X., Karkalas J., Hydrolysis of native starches with amylases, Animal Feed Science and Technology, Volume 30, Issues 1-2, (2006), 39-54.

Trindade W.D.S., Santos R.G., Review on the characteristics of butanol, its production and use as fuel in internal combustion engines, Renewable and Sustainable Energy Reviews, 69 (2017), 642-651.

Ulbrich M., Lampl V., Flöter E., Impact of modification temperature on the properties of acid-thinned potato starch, Starch, Volume 68, Issue 9-10, 885-899.

Vamadevan V., Bertoft E., Structure-function relationships of starch components, Starch, 67 (2015), 55-68.

Vohra M., Manvar J., Manmode R., Pagdilwar S., Patil S., Bioethanol production:

Feedstock and current technologies, Journal of Environmental Chemical Engineering, Volume 2, Issue 1, (2014), 573-584.

Voloshin R.A., Radionova M.V., Zharmukhamedov S.K., Veziroglu T.N., Allakhverdiev S.I., Review: Biofuel production from plant and algal biomass, International Journal of Hydrogen Energy, 41 (2016), 17257-17273.

Xie F., Pollet E., Halley P.T., Averous L., Advanced Nano-biocomposites Based on Starch, Springer International Publishing Switzerland, (2014).

Yamaguchi D., Hara M., Starch saccharification by carbon-based solid acid catalyst, Volume 12, Issue 6, (2010), 1018-1023.

Yan H., Yang Y., Tong D., Xiang X., Hu C., Catalytic conversion of glucose to 5-hydroxymethylfurfural over SO_4^{2-}/ZrO_2 and SO_4^{2-}/ZrO_2-Al_2O_3 solid acid catalyst, Catalysis Communications, 10 (2009), 1558-1563.

Yang Y., Xiang X., Tong D., Hu C., Omar M.M.A., One-pot synthesis of 5-hydroxymethylfurfural directly from starch over $SO_4^{2-}/$ ZrO_2-Al_2O_3 solid catalyst, Bioresource Technology, Volume 116, (2012), 302-306.

Zabed H., Sahu J.N., Suely A., Boyce A.N., Faruq G., Bioethanol production from renewable sources: Current perspectives and technological progress, Renewable and Sustainable Energy Reviews, 71 (2017), 475-501.

Zajsek K., Gorsek A., A kinetic study of sucrose hydrolysis over Amberlite IR-120 as a heterogeneous catalyst using in situ FTIR spectroscopy, Reaction Kinetic Mechanism Catalyst, 100 (2010), 265-276.

Zhang X., Zhang Z., Wang F., Wang Y., Song Q., Xu J., Lignosulfonate-based heterogeneous sulfonic acid catalyst for hydrolyzing glycosidic bonds of polysaccharides, Journal of Molecular Catalysis A: Chemical, Volume 337, (2013), 102-107.

APPENDIX A

DETAILS ABOUT HYDROLYSIS OF STARCH EXPERIMENTS

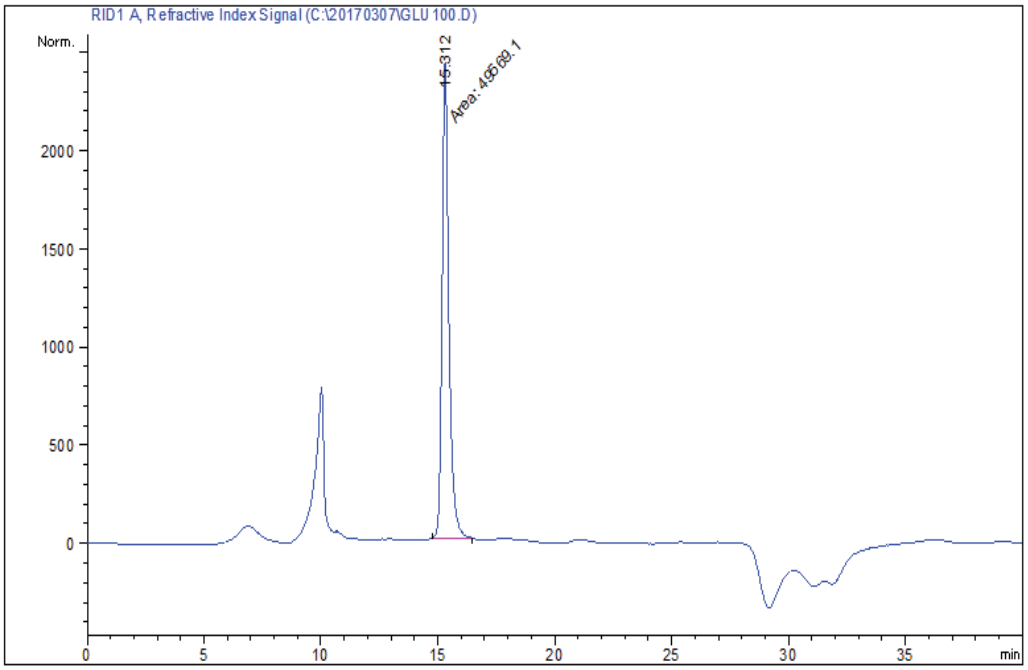

Figure 20. HPLC chromatogram of glucose (100 ppm)

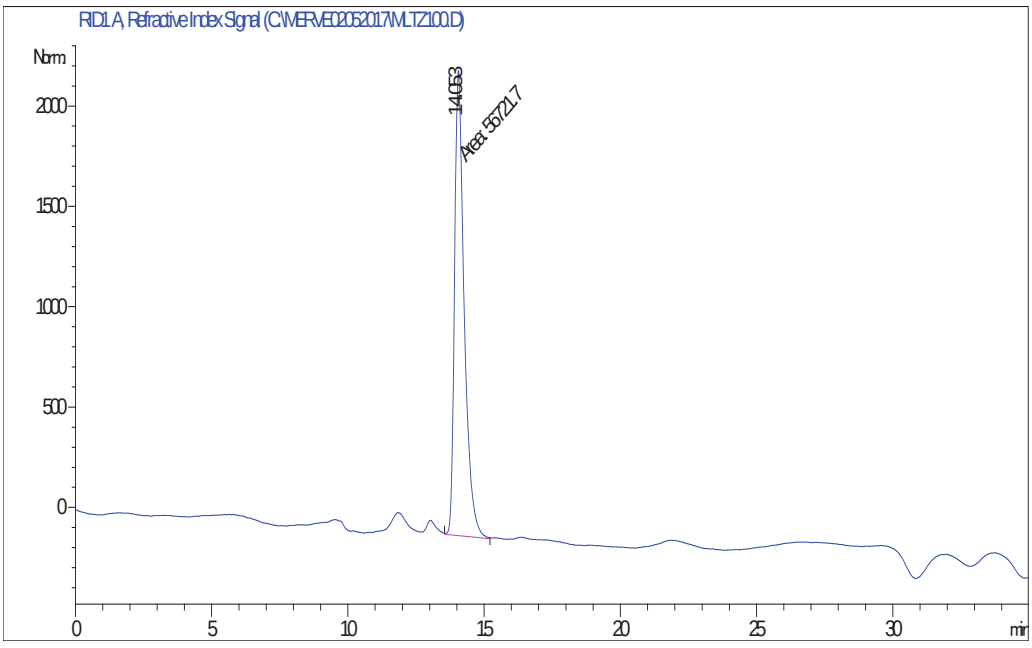

Figure 21. HPLC chromatogram of maltose (100 ppm)

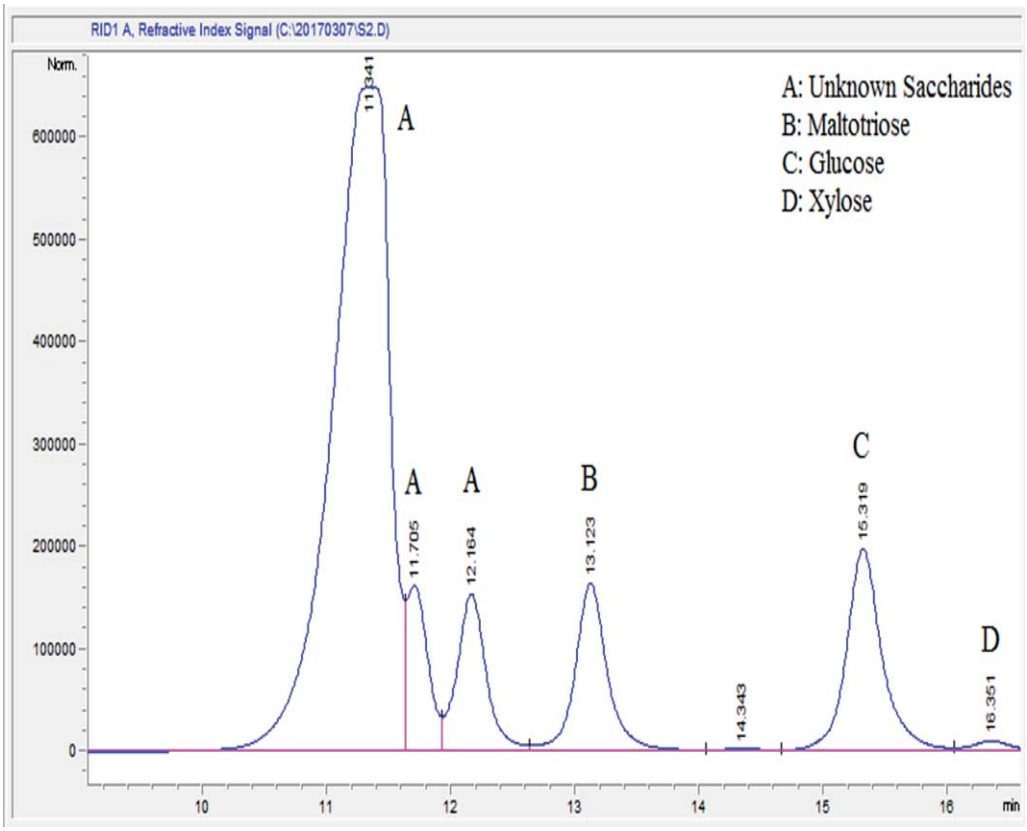

Figure 22. Retention times of products

Table 7. HPLC product area for 1%Ni/ 30% SiO_2- 70%Al_2O_3 catalyst calcinated at 700 ^{0}C for 6h

#	Time	Area	Height	Width	Area%	Symmetry
1	11.341	22954396	650808.2	0.5325	69.180	1.323
2	12.164	2547483.3	151452.4	0.2654	7.678	0.879
3	13.124	3037739.3	161416	0.2887	9.155	0.826
4	14.345	79373.9	2857.1	0.3932	0.239	0.981
5	15.32	4049312.3	193992.8	0.3126	12.204	0.82
6	16.351	289827.9	10371.1	0.3952	0.873	0.641

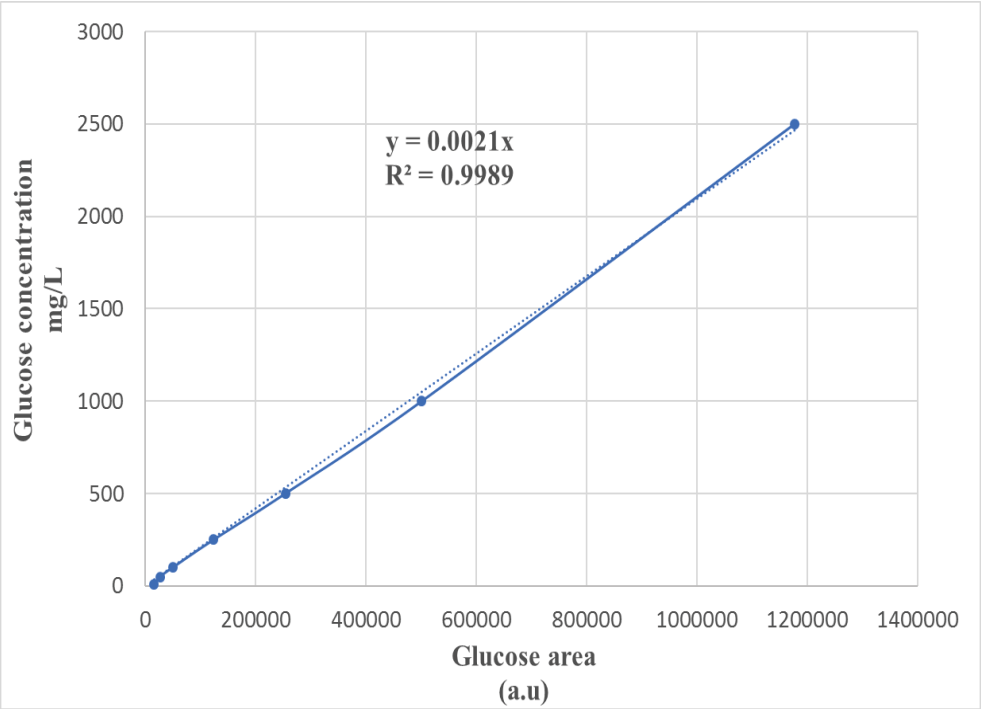

Figure 23. Glucose calibration curve

Table 8. Area percentage of products for Ni/SiO_2-Al_2O_3 catalyts

Catalysts Ni/SiO_2-Al_2O_3	**Glucose area percentage**	**Xylose area percentage**	**Maltorioz area percentage**	**Unknown saccharides Percentage**
1/30-70 & 700°C	12.2	0.9	7.7	79.2
1/70-30 & 700°C	1.6	0.0	1.0	97.6
10/30-70 & 700°C	1.9	0.0	1.9	96.4
10/70-30 & 700°C	0.6	0.0	0.4	99.0
5.5/30-70 & 500°C	3.1	0.0	2.9	94.0
5.5/70-30 & 500°C	5.5	0.0	4.8	89.7
5.5/30-70 & 900°C	0.1	0.0	0.0	99.9
5.5/70-30 & 900°C	2.6	0.0	1.0	96.3
1/50-50 & 500°C	11.1	0.0	7.9	81.0
10/50-50 & 500°C	10.3	1.4	8.3	79.3
1/50-50 & 900°C	0.1	0.0	0.0	99.9
10/50-50 & 900°C	0.0	0.0	0.0	100.0
5.5/50-50 & 700°C	7.6	0.0	6.5	85.5
5.5/50-50 & 700°C	-	-	-	-
5.5/50-50 & 700°C	7.2	0.0	0.4	92.4

Table 9. Concentration of products for Ni/SiO_2-Al_2O_3 catalysts

Catalysts Ni/SiO_2-Al_2O_3	**Glucose** (mg/L)	**Xylose** (mg/L)	**Maltorioz** (mg/L)
1/30-70 & 700°C	8454	849	5592
1/70-30 & 700°C	705	-	433
10/30-70 & 700°C	1062	-	1062
10/70-30 & 700°C	223	-	171
5.5/30-70 & 500°C	1725	-	1612
5.5/70-30 & 500°C	2685	-	2324
5.5/30-70 & 900°C	27	-	-
5.5/70-30 & 900°C	570	-	223
1/50-50 & 500°C	6146	-	4392
10/50-50 & 500°C	6223	1160	4682
1/50-50 & 900°C	17	-	-
10/50-50 & 900°C	0	-	-
5.5/50-50 & 700°C	3729	262	1549
5.5/50-50 & 700°C	-	-	-
5.5/50-50 & 700°C	4084	-	-

Table 10. Area percentage of products for Ni/ZnOTiO$_2$ catalyts

Catalysts Ni/ZnO-TiO$_2$	**Glucose area percentage**	**Unknown Saccharides area percentage**
1/10-90 & 400°C	0.0	100.0
1/50-50 & 400 °C	0.0	100.0
10/10-90 & 400°C	0.1	99.9
10/50-50 & 400°C	0.1	99.9
5.5/10-90 & 300°C	0.0	100
5.5/50-50 & 300°C	0.0	100
5.5/10-90 & 500°C	0.0	100
5.5/50-50 & 500°C	0.0	100
1/30-70 & 300°C	0.0	100
10/30-70 & 300°C	0.0	100
1/30-70 & 500°C	0.0	100
10/30-70 & 500°C	0.0	100
5.5/30-70 & 400°C	0.0	100
5.5/30-70 & 400°C	0.1	99.9
5.5/30-70 & 400°C	0.0	100